A diverse panel of 755 bread wheat accessions harbors untapped genetic diversity in landraces and reveals novel genetic regions conferring powdery mildew resistance

Rebecca Leber (0009-0005-7382-6406)[1], Matthias Heuberger (0000-0003-3283-9233)[1], Victoria Widrig (0000-0002-1285-3815)[1,2], Esther Jung (0009-0001-7470-2967)[1], Etienne Paux (0000-0002-3094-7129)[3,4], Beat Keller (0000-0003-2379-9225)[1]* & Javier Sánchez-Martín (0000-0002-0284-7219)[1,2]*

[1] University of Zurich, Department of Plant and Microbial Biology, Zollikerstrasse 107, 8008 Zurich, Switzerland

[2] Department of Microbiology and Genetics, Spanish-Portuguese Institute for Agricultural Research (CIALE), University of Salamanca, 37007 Salamanca, Spain

[3] Université Clermont Auvergne, INRAE, GDEC, 63000 Clermont-Ferrand, France

[4] VetAgro Sup Campus agronomique, 63370 Lempdes, France

* Corresponding authors

E-mail: j.sanchezmartin@usal.es, bkeller@botinst.uzh.ch

Key Message

A bread wheat panel reveals rich genetic diversity in Turkish, Pakistani, and Iranian landraces and novel resistance loci to diverse powdery mildew isolates via subsetting approaches in association studies.

Abstract

Wheat breeding for disease resistance relies on the availability and use of diverse genetic resources. More than 800,000 wheat accessions are globally conserved in gene banks, but they are mostly uncharacterized for the presence of resistance genes and their potential for agriculture. Based on the selective reduction of previously assembled collections for allele mining for disease resistance, we assembled a trait-customized panel of 755 geographically diverse bread wheat accessions with a focus on landraces, called the LandracePLUS panel. Population structure analysis of this panel based on the TaBW35K SNP array revealed an increased genetic diversity compared to 632 landraces genotyped in an earlier study and 17 high-quality sequenced wheat accessions. The additional genetic diversity found here mostly originated from Turkish, Iranian and Pakistani landraces. We characterized the LandracePLUS panel for resistance to ten diverse isolates of the fungal pathogen powdery mildew. Performing genome-wide association studies and dividing the panel further by a targeted subsetting approach for accessions of distinct geographical origin, we detected several known and already cloned genes, including the *Pm2a* gene. In addition, we identified 22 putatively novel powdery mildew resistance loci that represent useful sources for resistance breeding and for research on the mildew-wheat pathosystem. Our study shows the value of assembling trait-customized collections and utilizing a diverse range of pathogen races to detect novel loci. It further highlights the importance of integrating landraces of different geographical origins into future diversity studies.

Keywords

wheat landraces; genetic diversity; resistance genes; powdery mildew; plant-microbe interaction; genome-wide association mapping

Acknowledgments

We would like to thank Nikolaos Minadakis, Benjamin Jaegle, Zoe Bernasconi, Alexandros Sotiropoulos, Thomas Wicker, Bruno Studer and Anne Roulin for their input and guidance in acquiring necessary techniques for this study. We would further like to thank Sarah Furrler, Garp Linder and Pietro Sassi for their contributions to this project in the lab. This project was financially supported by the University of Zurich, Swiss National Science Foundation grants 310030_204165 and 310030B_182833 to B.K. JSM is recipient of the grants "Ramon y Cajal" Fellowship RYC2021-032699-I, funded by MCIN/AEI/10.13039/501100011033 and by the "European Union NextGenerationEU/PRTR" and PID2022-142651OA-I00, funded by MCIN/AEI/10.13039/501100011033 and "European Union NextGenerationEU/PRTR".

53 **Introduction**

54 Bread wheat (*Triticum aestivum* L.) provides more calories and protein per person than any other crop on
55 Earth (FAO 2020). This allohexaploid (2*n* = 6*x* = 42, AABBDD) crop species originated from successive
56 hybridization events, where the latest polyploidization is thought to have occurred ~ 8,000 years ago in
57 the Fertile Crescent (Glémin et al. 2019; Haas et al. 2019). After domestication, wheat was disseminated
58 to Europe and Asia (Bonjean and Angus 2001), where accessions were selected based on the needs of
59 individual farmers, thus becoming locally adapted traditional accessions, so-called landraces (Zeven 1998;
60 Villa et al. 2005). With the Green Revolution in the 1960s, landraces were systematically replaced by
61 advanced cultivars (Evenson and Gollin 2003) at the cost of a narrower genetic diversity due to the
62 bottleneck effect of breeding (Tanksley and McCouch 1997; Reif et al. 2005). Consequently, modern
63 cultivars are likely to lack a substantial proportion of the genetic diversity present in the wheat gene pool
64 to combat abiotic and biotic stresses, including infection by pathogens. Plant diseases are a big threat to
65 agriculture, with fungal pathogens playing a major role, causing an estimated annual yield loss of 18% in
66 wheat (Savary et al. 2019). Among those, wheat powdery mildew, caused by the obligate biotrophic
67 ascomycete *Blumeria graminis* f.sp. *tritici* (*Bgt*), is a major source of yield loss worldwide (Savary et al.
68 2019). Chemical control via pesticides is expensive and can negatively impact the surrounding ecosystem
69 (Dormann et al. 2007; Bourguet and Guillemaud 2016). Besides, the European Commission proposed
70 binding rules to reduce EU pesticide usage by 50% until 2030 (EU 2020). Therefore, alternative strategies
71 are needed to control wheat mildew, especially in the context of climate change, as the geographical
72 dispersal of pathogens and the severity of their infections are expected to increase rapidly (Singh et al.
73 2023).

74 In the Farm-to-fork strategy, the deployment of disease-resistant wheat accessions is proposed as a
75 sustainable and effective way to combat pathogens (EU 2020). Such resistance can be conferred by
76 resistance (*R*) genes, which typically encode intracellular nucleotide-binding leucine-rich repeat receptors

77 (NLRs), albeit not always, that recognize pathogen avirulence effector proteins (AVRs) (Dodds and Rathjen
78 2010; Sánchez-Martín and Keller 2021; Athiyannan et al. 2022b). *R* gene resistance acts in a race-specific
79 manner when an R protein recognizes the corresponding AVR (Flor 1971; Dodds and Rathjen 2010). The
80 over 90 genetically characterized *R* genes against powdery mildew (*Pm* genes) represent a cornerstone of
81 wheat breeding (McIntosh et al. 2013). However, race-specific resistance can be rapidly overcome by
82 pathogens by evolving AVRs to evade recognition (McDonald and Linde 2002; Mundt 2014; Brown 2015).
83 Due to this constant arms race and the low efficacy of the currently cloned *Pm* genes (Dracatos et al.
84 2023), the identification of new resistance genes is needed for wheat breeding programs. More than 7,000
85 distinct NLR-encoding genes are estimated to be present in the wheat gene pool (Walkowiak et al. 2020).
86 Based on this genomic analysis, there are possibly hundreds of potentially active but unknown *Pm* genes
87 in the wheat germplasm. The untapped genetic diversity of wheat landraces and their adaptation to
88 individual environments with high disease pressure of locally adapted pathogens makes them promising
89 candidates for containing such genes (Tanksley and McCouch 1997; Zeven 1998; Müller et al. 2018).

90 Together with cultivars and wild relatives, landraces are conserved in gene banks, where, to date, more
91 than 800,000 *Triticum* accessions are stored (CGIAR 2023). However, these remain mostly uncharacterized
92 for their potential in agriculture and their adaptive mechanisms are poorly understood, limiting their use
93 in breeding (Tanksley and McCouch 1997; Müller et al. 2018). Attempts to unlock this hidden potential
94 have been made using different approaches. For example, Balfourier et al. focused on maximizing the
95 representation of different breeding statuses, dates of registration and geographical origin to reduce the
96 collection size of the INRAe bread wheat collection from about 12,000 to 4,506 accessions (Balfourier et
97 al. 2019). Genotyping these accessions improved understanding of wheat phylogeography and genetic
98 diversity over time. Another study characterized the genetic diversity of 80,000 accessions, which
99 represented a large part of the CIMMYT and ICARDA germplasm banks, covering not only domesticated
100 hexaploid wheat but also tetraploids and crop wild relatives (Sansaloni et al. 2020). This revealed

101 unexplored diversity in landraces and wheat selection footprints. In a third recent example, Schulthess et
102 al. genotyped the IPK winter wheat collection of 7,651 accessions and a reference panel of 325 European
103 elite cultivars (Schulthess et al. 2022). Later, this collection was phenotyped with a single powdery mildew
104 isolate, detecting eleven previously undescribed resistance loci (Hinterberger et al. 2022).

105 Here, we used a panel based on former bread wheat collections assembled for allele mining (Bhullar et al.
106 2009, 2010b). These former collections included a main panel selected using a focused identification of
107 germplasm strategy (FIGS) approach, revealing accessions with potentially high selection pressure for
108 powdery mildew resistance (Mackay and Street 2004; Bhullar et al. 2009). We have now reduced these
109 collections, focusing on landraces and maximizing the diversity of geographical origin. The reduced size of
110 the panel allowed us to phenotype it with a diverse set of ten *Bgt* isolates, constituting a trait-customized
111 panel that is ideal for searching for powdery mildew-resistant accessions and the underlying genes
112 (Mascher et al. 2019). Using genome-wide association studies (GWAS) and a targeted subset approach for
113 accessions of shared geographical origin and isolate-specific resistance patterns, we detected 22 most
114 likely novel genetic regions associated with powdery mildew resistance.

115 **Materials and Methods**

116 Plant material and growth conditions

117 As starting material from which we selected our working panel, we utilized a formerly assembled bread
118 wheat collection of 1,320 landraces that had been selected based on FIGS of accessions with potentially
119 high selection pressure for powdery mildew resistance (Bhullar et al. 2009). Later, this collection was
120 complemented with 733 accessions of diverse geographical origins (Bhullar et al. 2010b). Assessment of
121 accession type, i.e., landrace, cultivar, breeding/research material or unknown, was based on passport
122 data at https://www.genesys-pgr.org. When no GPS data was available for collection sites of accessions,
123 we projected GPS using https://maps.google.com from the most detailed description available, i.e., given

124 villages up to countries. Accessions from the two combined wheat collections were phenotyped for
125 powdery mildew resistance at seedling stage with the six *Bgt* isolates CHE_94202, CHE_96224,
126 CHE_97223, CHE_97266, CHE_98230 and GBR_JIW2. The infection phenotype was used to create a
127 reduced panel of wheat accessions, consisting of approximately 50% that showed complete resistance
128 (0% visible infection) to one or more isolates, or resistance with a threshold of 20% to at least two isolates.
129 The remaining 50% were susceptible to all six isolates and had the same ratio of spring wheat to winter
130 wheat as the resistant part of the panel. Additionally, we used wheat accession origin as a proxy for
131 relatedness, choosing a geographically close susceptible counterpart for each resistant accession. The
132 resulting diverse LandracePLUS panel of 755 bread wheat accessions (Table S1), with a focus on the fertile
133 crescent, was infected with four additional *Bgt* isolates at seedling stage, i.e., CHE_19004, CHN_46_30,
134 ISR_106 and ISR_94.

135 Differential lines used to assess virulence patterns for 27 different *Pm* genes are shown in Table S2,
136 including near-isogenic lines (NILs) and accessions containing the designated gene. NILs had been
137 backcrossed multiple times with susceptible accessions "Federation" or "Chancellor", depicted by
138 /x*Accession, where x is the number of backcrosses to the designated accession (McIntosh et al. 2013).
139 Other differential lines were used as original seeds from the USDA ARS (https://npgsweb.ars-
140 grin.gov/gringlobal/search) or propagated using isolation bags per single spikes.

141 Seeds used for infection tests were obtained by propagating accessions in the field using single rows per
142 genotype without isolation. Seedlings for infection tests were grown in 40-well plastic trays in a growth
143 chamber cycled at 20°C/16°C, 16/8h photoperiod with 80% relative humidity.

144 Powdery mildew isolates and infections

145 We used previously sampled and sequenced *Bgt* isolates CHE_94202, CHE_96224, CHE_97223,
146 CHE_97266, CHE_98230, CHN_46_30, GBR_JIW2, ISR_94 and ISR_106, which are described by

147 Sotiropolous (Sotiropoulos et al. 2022). We sampled chasmothecia of one additional isolate, CHE_19004,
148 in 2019 from a wheat field at Reckenholz, Affoltern, Switzerland, which was revived and sequenced as
149 previously described (Sotiropoulos et al. 2022).

150 Powdery mildew infection tests of the differential lines and the LandracePLUS panel accessions were
151 carried out on the primary leaves of ten to fifteen-day-old seedlings grown under the abovementioned
152 conditions. Leaf segments were placed with their adaxial side up in Petri dishes filled with 0.5% Phyto agar
153 containing 30 ppm benzimidazole. Fresh conidiospores were dispersed using 5 ml Pasteur glass pipettes
154 in a settling tower (Lutz et al. 1992). Petri dishes with detached leaf segments were incubated for seven
155 to nine days at 20°C, 80% relative humidity with a 16 h light/8 h dark cycle and 50 µmol $m^{-2}s^{-1}$ photon flux
156 density. Infections were done in batches, with replicates of leaf segments from at least three independent
157 seedlings per wheat accession on the same petri dish, infected at the same time. We used mildew
158 susceptible accession Kanzler as a control for a proper mildew infection for all infection tests. Accessions
159 Chancellor and Federation were used as additional susceptible controls for tests on differential lines.
160 These susceptible controls were grown together with the tested accessions of each batch and distributed
161 throughout the layout petri dish. If controls were not well infected and, in addition, the overall infection
162 was low, the full infection test was repeated rather than using controls as a means to correct phenotypic
163 values.

164 Disease levels were assessed seven to nine days after inoculation, depending on fungal growth in the
165 batch, using a discrete quantitative scale with a score from 0 to 100 for the percentage of leaf area covered
166 by sporulating mildew colonies, as described earlier by Kaur (Kaur et al. 2008). Disease levels of differential
167 lines were directly scored as resistant (<=20) and susceptible (>20).

168 <u>DNA extraction and genotyping</u>

169 DNA extraction of plant material was performed as previously described (Stein et al. 2001). DNA quality
170 was assessed via agarose gels and genotyped using the TaBW35K single nucleotide polymorphism (SNP)
171 array (Paux et al. 2022). The SNP call dataset included marker positions and flanking sequences based on
172 RefSeq v1.0 of Chinese Spring (IWGSC 2018).

173 *Pm* gene screening via polymerase chain reactions (PCRs) and sequencing

174 PCR analysis was performed using *Pm4* (Sánchez-Martín et al. 2021) and *Pm2* haplotype-specific markers
175 (Manser et al. 2021). Four random landraces that were identified to carry *Pm2* were then used for long-
176 range and a following nested PCR to amplify the gene for Sanger sequencing as previously described
177 (Sánchez-Martín et al. 2016).

178 General data analysis and visualization

179 Unless indicated otherwise, analyses were done using R version 3.6.3 (R Core Team 2022), including data
180 handling with Tidyverse (Wickham et al. 2023) and visualizations with R package ggplot2 version 3.3.6
181 (Wickham 2016).

182 Kinship matrices for hierarchical clustering and visualization were done with GAPIT version 3 (Wang and
183 Zhang 2021). Dendrogram formation and hierarchical clustering were performed using the stats R package
184 version 3.6.3 (R Core Team 2022) functions hclust (method = ward.D2) and dist (method = euclidean).
185 Defining clusters of genotypes was done using the package dendextend version 1.16.0 (Galili 2015).

186 Wheat *Pm* gene sequence assembly and alignment was done with CLC Genomics Workbench version
187 20.0.4 (Qiagen Bioinformatics, https://digitalinsights.qiagen.com/). Pathogen *Avr* gene sequence
188 alignment was done using IGV version 2.15.4 (Robinson et al. 2011).

189 SNP filtering and file format

190 We filtered for “PolyHighResolution” or off-target variants (OTVs) and markers with known chromosomal
191 positions in the Chinese Spring RefSeq v1.0 reference genome. Thresholds of 25% heterozygosity, 25%
192 missing data per wheat accession and 5% missing data per marker were applied, and markers with
193 duplicated positions were removed. Absent haplotypes of an OTV were translated to “NA” to facilitate
194 their inclusion in downstream analyses. Taken together, this resulted in 29,965 polymorphic markers.
195 These were brought into a Hapmap format with R and then transformed into a variant call format (VCF)
196 file using the software TASSEL version 5.0 (Bradbury et al. 2007). This file was used as an input to generate
197 plink files using vcftools version 0.1.16 (Danecek et al. 2011), which were then transformed together with
198 phenotyping data into .bed, .bim and .fam files using PLINK v1.07 (Purcell et al. 2007) for Admixture and
199 association analyses.

200 Phenotypic data analysis

201 The raw median of the biological replicates was taken as the final phenotype for seedling resistance
202 assessment. Inconclusive phenotypes, e.g., 50% resistant and 50% susceptible against the same isolate
203 due to possible seed contamination or heterozygosity, were excluded from further analyses. Phenotypes
204 with less than three replicates were also excluded. These values were transformed into two categories,
205 where 0-20% = resistant and >20% = susceptible for GWAS and Mantel tests. For Pearson correlation,
206 phenotypic values of the differential lines were transformed to 0 and 1, respectively.

207 Pearson correlation between the isolate phenotypes was calculated using the stats package and visualized
208 with the package corrplot version 0.92 (Wei and Simko 2021). Heritability was calculated for each
209 pathogen isolate using R package lme4 version 1.1-34 (Bates et al. 2015) and a nested linear mixed model
210 approach, where fixed variance is defined as the wheat genotype, and random variance as the infection
211 test batch (“Round”) nested within the specific petri dish (“Plate”). P-values are based on ANOVA tests
212 between the full and null models.

213 *In silico* genotyping of TaBW35K array SNP variants in high-quality sequenced wheat genomes

214 For the comparison of genetic diversity, Fielder (Sato et al. 2021), Renan (Aury et al. 2022) and the 10+
215 wheat reference genomes ArinaLrFor, Chinese Spring, Claire, Cadenza, Jagger, Julius, Landmark, Lancer,
216 Mace, Paragon, Norin61, Robigus, Stanley, SYMattis and Weebill (IWGSC et al. 2018; Walkowiak et al.
217 2020) were added. Flanking sequences of SNP array markers were queried using BLASTN searches against
218 the publicly available wheat genomes. Blast results were filtered for hits with at least 60bp alignment and
219 96% shared identity, allowing no more than three mismatched nucleotides. Positions of the SNPs were
220 then extracted from BLASTN alignments on the respective genomes through in-house scripts. Merging the
221 resulting dataset with the 29,965 previously used markers resulted in an overlap of 27,337 SNPs used for
222 principal component analysis (PCA) and hierarchical cluster analysis.

223 Diversity Analysis via PCA and hierarchical clustering

224 PCAs for the LandracePLUS panel and high-quality sequenced genomes were done based on the 27,337
225 SNP set using the R package SNPRelate version 1.18.1 and gdsfmt version 1.20.0 (Zheng et al. 2012). For
226 the PCA for the comparison to the 632 landraces from the INRAe study (Balfourier et al. 2019), we first
227 filtered the genotyping data of the combined datasets provided by INRAe for the same cleaned 29,965
228 SNPs of the LandracePLUS panel. Because no creation of a Hapmap or VCF file was necessary for further
229 downstream analysis, this dataset could be directly used for PCA using the prcomp function.

230 Hierarchical clustering analysis was performed using the kinship matrix of the 27,337 SNP set, including
231 high-quality sequenced genomes. We visualized the dendrogram using dendextend version 1.16.0 (Galili
232 2015).

233 Admixture kinship analysis and comparative visualization

234 We used the .bed file of 29,965 SNPs (not including the chromosome-assembled genomes) as an input to
235 assess population structure using ADMIXTURE version 1.3.0 (Alexander et al. 2009), where the most likely
236 number of founder populations K can be estimated via running the model over a series of values of K and
237 then choosing K around the lowest occurring cross-validation (CV) error. We ran the model for K = 2 to K
238 = 20. However, the CV error steadily dropped with increasing K (Fig S1). We, therefore, regarded Ks after
239 the largest CV error drops of 33% in total as appropriate estimations for population structure, i.e., K = 4
240 to K = 6. A bootstrap of 500 and CV of 10 was used for this analysis.

241 A kinship matrix for the visualization was made with the same 29,965 SNP set using GAPIT version 3 (Wang
242 and Zhang 2021). The kinship matrix was used as an input for hierarchical clustering for the comparative
243 dendrogram. This dendrogram was visualized using the R package ggdendro version 0.1.23 (de Vries and
244 Ripley 2022). Finally, these two plots and the admixture barplot were merged using the R package
245 patchwork version 1.1.1 (Pedersen 2020).

246 Mantel test

247 To calculate the Mantel test, we first transformed the VCF file of 29,965 SNPs into genlight format using
248 the R package vcfR version 1.14.0 (Knaus and Grünwald 2017). Then, we used this as an input for
249 producing a Bray-Curtis genetic distance matrix with the vegdist function from R package vegan 2.6-4
250 (Oksanen et al. 2022). This genetic matrix was then correlated to the Euclidean phenotypic distance
251 matrices using the vegan package mantel function with the Spearman method and 999 permutations to
252 obtain Mantel r values.

253 Genome-wide association analysis (GWAS)

254 For GWAS, missing data from the 29,965 SNP set was imputed using general Beagle version 5.4 (Browning
255 et al. 2018). GWAS and estimates of effect size – beta – were calculated using the GEMMA (Zhou and
256 Stephens 2012) univariate linear mixed model. For the full LandracePLUS panel and each subset, .bed,

257 .bim and .fam files were created as described above. .fam files were used as input for creating the kinship
258 matrix in GEMMA using the options -gk 1 and -miss 1 . MAF was set to 1% for the full LandracePLUS panel
259 and all subsets above 300 accessions in size, while for the other runs the MAF was set to 5%. This matrix
260 was then integrated into the univariate linear mixed model with option -miss 1 (Zhou and Stephens 2012).
261 Phenotypic data for the association studies was added to the .fam in R. P-values were based on the
262 likelihood ratio test, and -log10 transformed for Manhattan plots. We used two thresholds to account for
263 multiple testing: the False Discovery Rate (FDR) and the more conservative Bonferroni correction (BC).
264 However, we regarded SNPs that passed the FDR test as significant.

265 Due to the design of the TaBW35K SNP array based on linkage disequilibrium (LD), meaningful LD decay
266 analysis was not possible. We, therefore, decided to define GWAS peak intervals based on the LD decay
267 results of a recent study on bread wheat using over 40 million SNPs (Liu et al. 2023). There, LD decay was
268 found to be 6.0353, 2.3851 and 3.0278 Mb for subgenomes A, B and D, respectively. Hence, we defined
269 peaks in a subgenome-dependent manner, as regions where at least two SNPs were significantly
270 associated with the powdery mildew phenotype within the range of the above LD decay bp distances. We
271 further considered significant single SNP associations as peaks if they uniquely mapped to one
272 chromosome (weak homology on homoeologs, i.e., at least six additional SNPs/gaps), were surrounded
273 by no or few SNPs and (1) they occurred for more than one isolate or (2) their significance passed the
274 more stringent BC threshold. The most significant SNP – the peak SNP – plus/minus the subgenome-
275 specific LD decay distance was used to define each peak interval. Alternatively, if several peak SNPs
276 occurred, both were used for the interval calculation.

277 To test if the peak on chromosome 5D was derived from *Pm2* and account for its presence, we included a
278 covariate (option –c) for binary information on the presence of *Pm2* based on haplotype-specific PCR
279 screening.

280 Random subsets were produced using R package tibble 3.1.8 (Müller and Wickham 2022). Subsets of
281 geographical origin were based on countries of origin.

282 The physical position of previously described *Pm* genes was either taken from the corresponding
283 publication when available or estimated by blasting the flanking markers using BLASTN against Chinese
284 Spring RefSeq v1.0 as a reference.

285 Accessions that possibly carry the causal genes of a resistance-associated region were determined by 1)
286 having at least 50% of the resistance-associated SNPs within an associated region and 2) being resistant
287 to the respective isolate (<=20% leaf coverage).

288

289 **Results**

290 We assembled a geographically diverse panel of 755 bread wheat accessions (Fig 1a-c) based on the
291 selective reduction of former collections used for allele mining of the powdery mildew resistance gene
292 *Pm3* (Bhullar et al. 2009, 2010b). In the selection process, we focused on landraces and combined data on
293 geographical origin with phenotypes of powdery mildew seedling stage resistance to six *Bgt* isolates. The
294 resulting panel, hereafter LandracePLUS panel, contains 521 winter wheat and 234 spring wheat
295 accessions, including 576 landraces, 162 older cultivars (acquisition date from 1946 to 2003, with the main
296 part from the 60s and 70s), seven research or breeding lines and eleven unknown accessions (Table S1).
297 We used the LandracePLUS panel, which covers a broad geographical distribution, with a focus on
298 accessions originating from the Middle East (Fig 1a-b), to detect genetic loci associated with resistance to
299 the powdery mildew pathogen (Fig 1d).

300 <u>Diversity analysis of the LandracePLUS panel reveals unexplored genetic diversity</u>

A total of 29,965 high-quality, polymorphic SNPs derived from genotyping with the TaBW35K SNP array were used for diversity analysis. All these SNPs had known chromosomal positions based on the Chinese Spring reference genome assembly RefSeq v1.0 (IWGSC 2018), including 18,610 regular SNPs and 11,355 OTVs, i.e. markers that detect both presence-absence polymorphisms and nucleotide polymorphisms. The 29,965 markers were distributed across the wheat genome, similar to earlier findings (Liu et al. 2017; Alemu et al. 2021; Govta et al. 2022), with lower coverage of genome D compared to the A and B genomes: 11,684 (39.0%) markers on the A-genome, 13,589 (45.3%) on the B-genome and 4,692 (15.7%) on the D-genome. On average, 1,427 markers were assigned per chromosome, resulting in an average density of one marker each 483 Kbp. The least markers were assigned to chromosome 1D and most to chromosome 2B, with 497 and 2,465 markers, respectively.

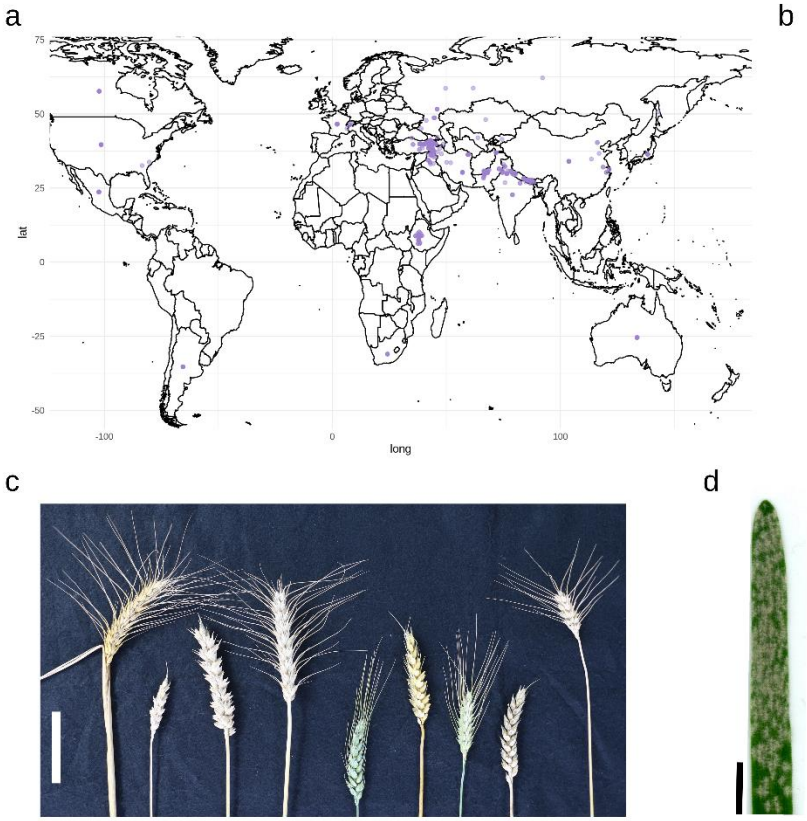

Country of origin	Number of accessions
Argentina	12
Armenia	8
Australia	14
Azerbaijan	1
Canada	8
Switzerland	4
China	45
Ethiopia	38
France	30
India	40
Iran	131
Iraq	19
Japan	18
Kazakhstan	1
Kyrgyzstan	1
Mexico	20
Nepal	40
Pakistan	42
Russia	13
Tajikistan	4
Turkey	231
USA	19
Uzbekistan	1
South Africa	4
unknown	11

Figure 1. LandracePLUS panel diversity and powdery mildew symptoms

313 **a** World map with semitransparent purple dots representing the origin of each of the 755 wheat accessions of the
314 LandracePLUS panel. **b** Number of accessions from the LandracePLUS panel per country of origin. **c** Selection of
315 diverse wheat ears from the LandracePLUS panel. Scale bar, 5 cm. **d** Leaf of wheat cultivar "Kanzler" with powdery
316 mildew symptoms. Scale bar, 1 cm

317 For a better interpretation of the observed genetic diversity within the LandracePLUS panel, wheat
318 accessions with high-quality genome sequences, namely the 10+ wheat reference genomes (IWGSC 2018;
319 Walkowiak et al. 2020), Fielder (Sato et al. 2021) and Renan (Aury et al. 2022) were included in the analysis
320 with 27,337 out of the 29,965 SNPs that mapped unambiguously to chromosomes of these genomes. Most
321 accessions with reference genomes available clustered in Group 2 of the LandracePLUS panel, while
322 Norin61 and Chinese Spring were on the edge of Group 4 (Fig 2a). A PCA (Fig 2a) and a dendrogram based
323 on hierarchical clustering analysis (Fig 2b) revealed four genetic clusters correlated with geographical
324 origin overall. Group 1 was dominated by accessions from Iran and Pakistan, while Group 2 was composed
325 of accessions of mixed origin (Ethiopia, South Africa, USA, Canada, Mexico, Argentina, France, Switzerland,
326 Kazakhstan, Kirgizstan, Tajikistan, Uzbekistan, Armenia and Russia). Group 3 predominantly contained
327 accessions from Turkey, and Group 4 was dominated by South, Southwest, and East Asia (Iraq, Azerbaijan,
328 India, Nepal, China and Japan).

329 When highlighting the different types of accessions in the PCA, landraces covered almost the entire
330 genetic diversity range of the LandracePLUS panel. In contrast, the 162 cultivars clustered mainly with
331 Group 2 and partially with Group 4 (Fig S2a). Therefore, landraces were genetically more diverse than
332 cultivars and clustered apart from them. However, this was not always the case, as shown by the example
333 of Ethiopian landraces, which clustered with cultivars in Group 2 (Fig S2b, Fig 2a), suggesting that Ethiopian
334 landraces have substantially contributed to breeding programs. The close clustering of accessions from all
335 over the world described above (Fig 2a-b) is likely driven by this separation between landraces and
336 cultivars. As most of these geographically diverse accessions clustering together are cultivars, their genetic
337 similarity is not derived from their origin but their breeding status as cultivars.

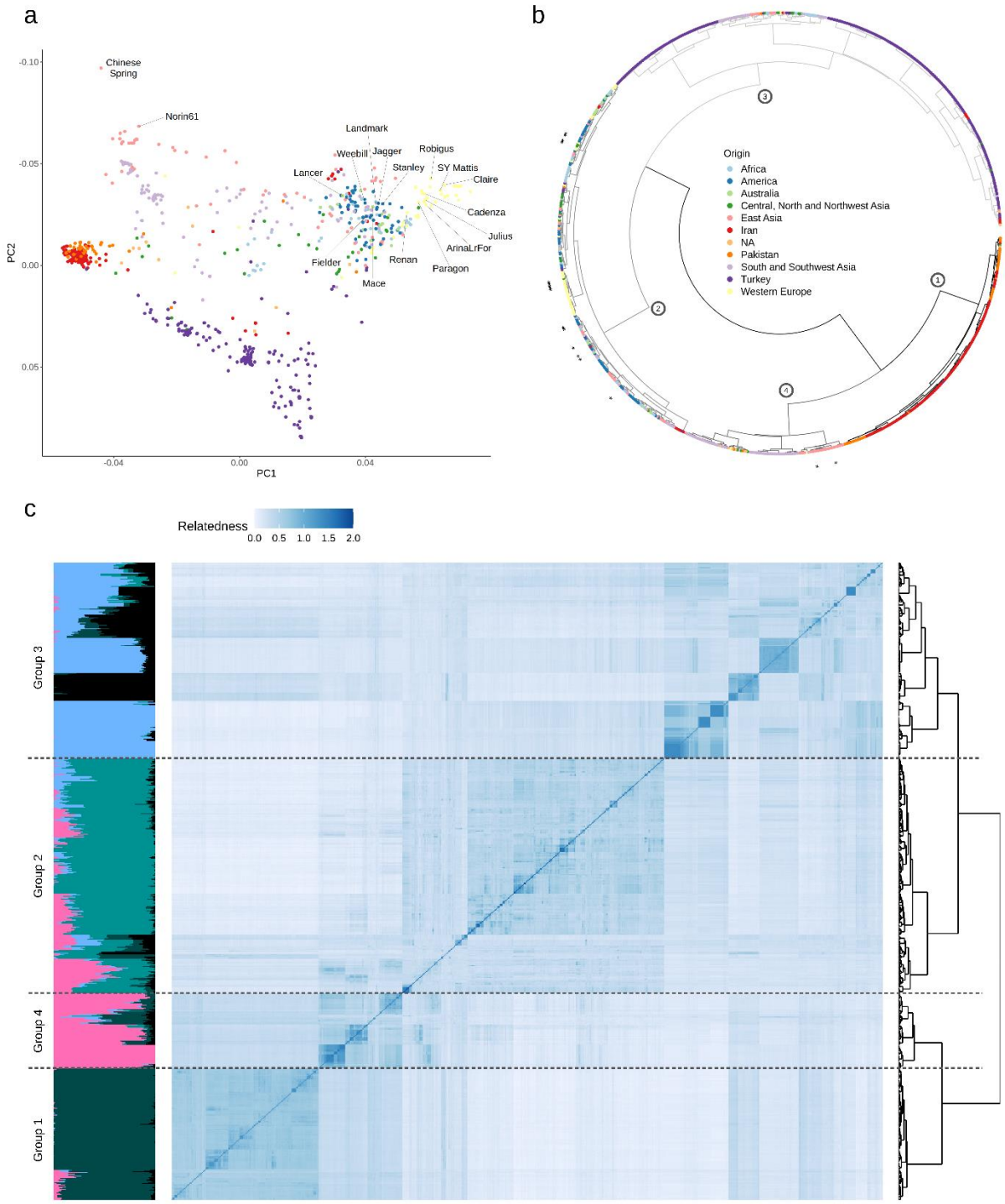

Figure 2. Genetic diversity and kinship analysis of the LandracePLUS panel

a PCA from 27,337 SNPs including high-quality sequenced wheat accessions labelled in the figure. PC1 = 8.4%, PC2 = 5.1%. Colors refer to the geographical origin of accessions and are indicated in b. **b** Dendrogram of a hierarchical clustering analysis from 27,337 SNPs including high-quality sequenced accessions indicated with stars. Colors

343 represent the geographical origin of wheat accessions. Circled numbers on nodes refer to Groups 1 to 4 when
344 dividing into four clusters. **C** Alignment of Admixture plot, kinship matrix and dendrogram for the 755 wheat
345 accessions based on 29,965 SNPs. The Admixture plot shows K=5, where colors represent ancestral populations. In
346 the kinship matrix, more saturated shades of blue indicate stronger relatedness. Dashed lines separate the four
347 groups based on hierarchical clustering

348

349 We assessed population structure performing hierarchical clustering on the 29,965 SNP set (excluding the
350 high-quality genome sequences) and compared it to a kinship matrix and Admixture analysis (Fig 2c). The
351 found clusters reflected the four groups described earlier, except for a shift of several accessions of
352 diverse origin from Group 3 to Group 2. Estimated ancestral populations K=5 revealed a good fit for the
353 LandracePLUS panel's diversity into four groups (Fig S1). Yet, the kinship matrix revealed additional
354 subdivisions within Groups 3 and 4.

355 To assess whether the LandracePLUS panel represents a similar genetic diversity compared to former
356 studies on wheat germplasm, we compared our data with a collection of 632 landraces that were
357 genotyped with the TaBW280K SNP array (Rimbert et al. 2018), which contains all markers that were used
358 for the LandracePLUS panel (Balfourier et al. 2019). A PCA with 29,965 filtered SNPs (Fig S3) showed that
359 the LandracePLUS panel covers the genetic diversity of this collection and further revealed unexplored
360 genetic diversity absent in the study of Balfourier and colleagues (Balfourier et al. 2019). This additional
361 diversity was mainly in Groups 1 and 3, comprising Turkish, Pakistani and Iranian landraces.

362 Taken together, the LandracePLUS panel is a diverse selection of wheat accessions with a pronounced
363 diversity of landraces compared to cultivars and high-quality sequenced genomes. Furthermore, the panel
364 covers earlier found genetic diversity and additionally expands it, mainly with Turkish, Pakistani and
365 Iranian landraces.

366 <u>Differential lines reveal diverse virulence in a set of ten powdery mildew isolates</u>

To maximize the chances of finding novel resistance genes, we first tested ten random isolates on a global collection of 27 differential lines, including NILs and donors of cloned or genetically described *Pm* genes (Fig 3). On average, isolates were avirulent on ten out of 27 differential lines. While isolates CHE_96224, CHE_97266 and CHE_98230 were avirulent on 16, 18 and 16 resistant differential lines, respectively, isolates CHE_19004 and ISR_94 were more virulent, with five and two resistant lines, respectively. Each isolate had a distinct virulence pattern, reflecting that the ten chosen mildew isolates represent broad diversity in virulence, confirmed by haplotype analysis of molecularly cloned *Avrs* (Table S3).

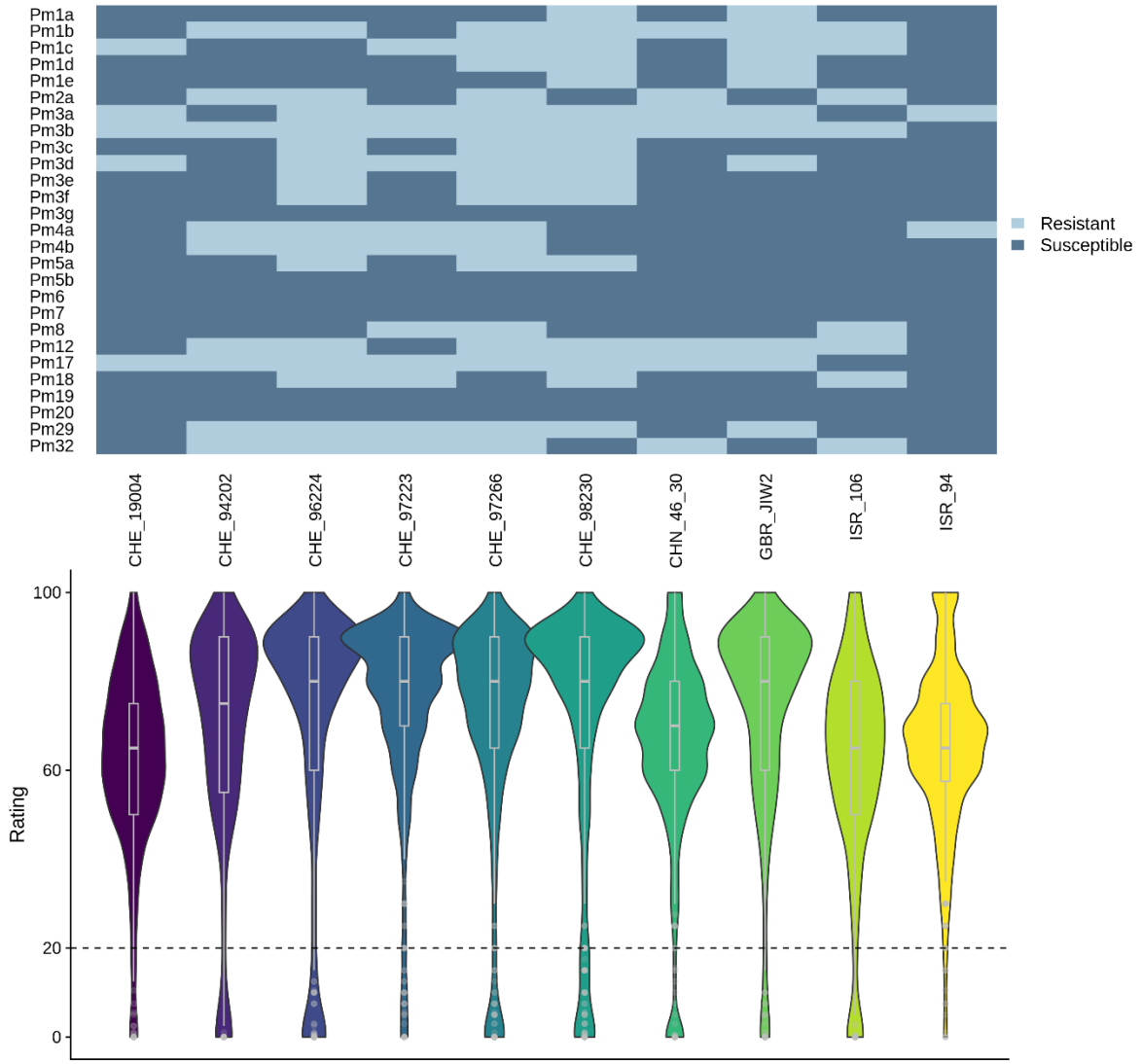

375 **Figure 3. Virulence patterns of powdery mildew isolates and resistance distribution in the LandracePLUS panel**

376 Virulence pattern of the ten powdery mildew isolates on differential lines with known *Pm* genes are shown as a
377 heatmap on the top. On the bottom, the virulence pattern of the ten powdery mildew isolates on the LandracePLUS
378 panel is depicted via violinplots and boxplots, highlighting median, 25 and 75 percentiles. The defined resistance
379 threshold of 20 is indicated by a dashed line. Differential lines for the 27 *Pm* genes are listed in Table S2

380

381 Taken together, the resistance patterns of the differential lines reveal a phenotypically diverse set of ten
382 powdery mildew isolates.

383 <u>The LandracePLUS panel shows varying resistance to ten wheat powdery mildew isolates</u>

384 The response of the 755 wheat accessions to the ten powdery mildew isolates revealed an overall
385 susceptibility, with an average of 56 resistant accessions (rating <=20) per isolate (Fig 3). Considering the
386 response to individual isolates, only 35, 36, 40 and 17 wheat accessions were resistant to CHE_19004,
387 CHE_97223, GBR_JIW2 and ISR_94, respectively. This reflected the broad virulence of CHE_19004 and
388 ISR_94 already found in the differential lines, while CHE_97223 and GBR_JIW2 seemed to be more virulent
389 on the LandracePLUS panel compared to the set of differential lines. On the other side, 91 and 89 wheat
390 accessions were resistant to CHE_96224 and CHE_98230, respectively, which were the most avirulent
391 isolates on the differential lines along with CHE_97266.

392 Phenotypic Pearson correlation between the isolates based on the set of differential lines corroborated
393 the diversity of virulence (Fig S4a), with an average correlation coefficient of 0.31. The most similar
394 isolates were CHE_96224 and CHE_97266, as well as CHE_98230 and GBR_JIW2, with a correlation of 0.69,
395 while the two most diverging, though not significantly, were ISR_106 and ISR_94 with a negative
396 correlation of 0.18. Pearson correlation between the isolates based on the LandracePLUS panel showed
397 patterns resembling the differential line phenotypes (Fig S4b). While the overall relation between isolates
398 was similar, several correlation coefficients differed notably, mostly involving ISR_106, GBR_JIW2 and

399 CHE_98230. This deviation could be caused by a different content of *Pm* genes in the LandracePLUS panel
400 compared to the differential set. With a coefficient of 0.36, however, the average correlation was similar.
401 The diversity in resistance reactions observed within the LandracePLUS panel against these Bgt isolates
402 suggests highly diverse effector content, highlighting the chances of finding novel resistance loci in the
403 LandracePLUS panel.

404 No wheat accession showed resistance to all ten isolates, while nine wheat accessions were resistant to
405 nine of the isolates. On average, excluding accessions susceptible to all tested isolates, wheat accessions
406 were resistant to three isolates.

407 We predicted the presence of known *Pm* genes in accessions of the LandracePLUS panel that matched the
408 pattern of the corresponding *Pm*-containing differential line. For example, 23 accessions of the
409 LandracePLUS panel had the same resistance pattern as the *Pm2a* differential line and, hence, are good
410 candidates for containing *Pm2a*. Indeed, 15 of these 23 accessions contained *Pm2* according to haplotype-
411 specific markers (Manser et al. 2021) (Table S1). However, the potential presence of several *Pm* genes in
412 the same accession can mask the resistance pattern of a specific *Pm* gene. This limits the use of differential
413 lines to analyze overlapping resistance patterns and to predict specific genes. Nevertheless, the
414 information on resistance patterns can be a useful tool to narrow down candidate accessions for the
415 presence of a *Pm* gene of interest.

416 <u>The LandracePLUS panel shows isolate-dependent heritability of mildew response phenotypes and low</u>
417 <u>correlation between phenotype and genetic relatedness</u>

418 We calculated the phenotypic heritability using a linear mixed model approach. The effect of the wheat
419 genotype on mildew resistance was isolate-dependent, between 0.38 for ISR_94 and 0.79 for CHE_96224,
420 and with a batch effect of 0.48 and 0.12, respectively (Table S4). This suggests that the observed response
421 to CHE_96224 is highly reproducible, while the batch seemed to have a strong influence on resistance

422 reaction for ISR_94. Half of the isolates (CHE_94202, CHE_96224, CHE_97223, CHE_97266 and GBR_JIW2)
423 had a heritability of 0.7 or higher, while ISR_94 was the only mildew isolate with a value below 0.5, possibly
424 indicating a mixture of powdery mildew races. Accordingly, we removed isolate ISR_94 from all
425 subsequent analyses. To account for this batch effect for the remaining isolates, and since the described
426 nature of *R* genes can be considered a binary one – resistant or susceptible – we decided to transform the
427 phenotypic scoring values of 0 to 100 to these two categories, with a threshold of 20 or higher for
428 susceptibility. Thus, differences between batches are weighted less, providing more reliable phenotypes
429 and GWAS results.

430 Using these categorized phenotypes, we further tested the correlation between the genetic relatedness
431 and the phenotype using a Mantel test (Mantel and Valand 1970). There were only slight differences
432 between the ten different isolates, and the correlations were close to zero, with Mantel r values ranging
433 from -0.001 to 0.029, although not significant for most isolates (Table S5). This suggests that the applied
434 approach of assembling the LandracePLUS panel minimized the effect of population structure on trait
435 variation. The LandracePLUS panel should, therefore, provide improved power when conducting GWAS
436 (Myles et al. 2009).

437 <u>Association studies for seedling resistance to wheat powdery mildew in the LandracePLUS panel reveal</u>
438 <u>previously cloned *Pm* genes as well as possibly novel genes</u>

439 We conducted GWAS with the phenotyping data obtained for each of the nine powdery mildew isolates
440 on the LandracePLUS panel with a MAF of 1%. We first tested for a good fit of the univariate linear mixed
441 model based on QQ plots, which was confirmed for all isolates except CHE_97223 (Fig S5). GWAS of the
442 other eight isolates revealed five genomic regions associated with wheat mildew resistance on
443 chromosomes 1A, 2B, 5D, 7A and 7D (Table 1, Fig S6). To account for LD, we defined a peak region by
444 adding the average LD decay distance per subgenome from a recent study in wheat (Liu et al. 2023) to

445 either side of the peak SNP. The most significant peak was located on chromosome 5D for the *AvrPm2*-
446 containing *Bgt* isolates CHE_94202, CHE_96224, CHE_97266, CHN_46_30 and ISR_106. When focusing on
447 one representative *AvrPm2*-containing isolate, ISR_106, the mildew resistance association spanned the
448 region from 40,919,172 to 46,974,772 bp of the short arm of chromosome 5D of Chinese Spring (Fig 4a-c)
449 and included the *Pm2* resistance gene locus (Sánchez-Martín et al. 2016). To test if the presence of *Pm2*
450 was responsible for the significant association, we screened the LandracePLUS panel with a *Pm2*
451 haplotype-specific marker (Manser et al. 2021) and found that out of 66 wheat accessions resistant to
452 ISR_106, 31 contained *Pm2*. In the whole panel, 39 accessions contained *Pm2*, of which 34 were landraces
453 (Table S1). Most of these 34 accessions were from Turkey, with three landraces from Russia, Pakistan and
454 Tajikistan (Fig 4f). GWAS with a covariate for *Pm2* presence resulted in the loss of the significant peak (Fig
455 4d), corroborating that the peak was indeed caused by *Pm2*. Sequencing of the amplified *Pm2* locus in
456 four randomly selected landraces that were positive for the haplotype marker uniformly revealed the
457 presence of the known allele *Pm2a* (Sánchez-Martín et al. 2016).

458 **Table 1. Powdery mildew associated regions detected in the LandracePLUS panel**

Chromosome	Position	Isolate	beta	*Pm* genes described on specific chromosome (arm)
1AS	306,708 – 12,377,308	CHE_98230	-0.14	***Pm3***(1)*, Pm17*(2)*, Pm25*(3)
1BL	610,940,301 – 615,710,501	CHE_96224*	-0.08	*Pm28*(4), *Pm39*(5)
2BL	707,987,645 – 722,628,991**	CHE_96224	-0.20	*Pm6*(6)*, Pm33*(7)*,* ***Pm51***(8)*, Pm52*(9)*, Pm57*(10)*, Pm62 (11),* ***Pm63***(12)*, Pm64*(13)*,* ***PmKN0816***(14)*,* ***PmLS5082***(15)*,* ***PmQ***(16)*, PmY39*(17)*,* ***pmYN99102***(18)*, MlAB10*(19)*, Mlzec1*(20), ***PMCG15-009***(21)
3BL	667,372,099 – 672,142,299	CHN_46_30*	-0.05	*Pm41*(22)*, PmHNK*(23)
3BL	701,911,458 – 706,681,658	CHE_97266*	-0.15	*Pm41*(22)*, PmHNK*(23)
5BL	647,102,735 – 651,872,935	CHN_46_30*	-0.21	*Pm36*(24)*, Pm53*(25)*, PmAS846*(26)*, Ml3D232*(27)
5DS	40,919,172 – 46,974,772	CHE_94202 CHE_96224 CHE_97266 CHN_46_30 ISR_106	-0.37 -0.26 -0.23 -0.39 -0.39	***Pm2***(28)*,* ***Pm46*** (29)*, Pm55*(30)
7AL	717,179,300 – 733,267,996	CHE_94202 CHE_97266 CHE_98230 GBR_JIW2	-0.22 -0.22 -0.24 -0.35	*Pm1* (31)*, Pm9* (32)*, Pm37*(33)*,* ***Pm59***(34)*,* ***Pm60***(35)*,* ***PmG16***(36)*,* ***MlIw72***(37)*,* ***Mlm2033***(38)*,* ***Mlm80***(38)*,* ***mlRd30***(39)*,* ***MlUM15***(40)*, PmU*(41)*, PmTb7A.1*(42)*, PmTb7A.2*(42)*,* ***MlIW172***(43)*,* ***MlWE18***(44)
7BS	68,921,370 – 73,691,570	CHE_96224*	-0.12	*Pm40(45), Pm47(46), mljy(47), mlsy(47)*
7DL	631,068,212 – 637,123,812	GBR_JIW2	-0.10	*Pm19(48), Pm29(49)*

459 Physical positions of GWAS peaks on Chinese Spring and the isolates detecting them. Values for beta are shown for
460 the SNP of each peak with the strongest effect size. If several isolates produce the same peak, beta is listed for each.
461 *Pm* genes are listed that were described on the same chromosomal arm or the same chromosome without a
462 specified arm arm. *Pm* genes described in an overlapping genomic interval with the GWAS peak are highlighted in
463 bold. * Usage of a covariate for *Pm2* in the regarding association. ** Region of significant association without
464 extension based on LD decay. (1) Yahiaoui et al. 2004, (2) Singh et al. 2018, (3) Shi et al. 1998, (4) Peusha et al. 2004,
465 (5) Lillemo et al. 2008, (6) Wan et al. 2020, (7) Zhu et al. 2005, (8) Zhan et al. 2014, (9) Wu et al. 2019, (10) Dong et
466 al. 2020, (11) Zhang et al. 2018, (12) Tan et al. 2019, (13) Zhang et al. 2019, (14) Wang et al. 2021, (15) Wu et al.
467 2022, (16) Li et al. 2020, (17) Zhu et al. 2006, (18) Mu et al. 2022, (19) Maxwell et al. 2010, (20) Mohler et al. 2005,

(21) Zhang et al. 2023, (22) Li et al. 2020a, (23) Xu et al. 2010, (24) Blanco et al. 2008, (25) Petersen et al. 2015, (26) Xue et al. 2012, (27) Zhang et al. 2010, (28) Sánchez-Martín et al. 2016, (29) Gao et al. 2012, (30) Zhang et al. 2016, (31) Hewitt et al. 2021, (32) McIntosh et al. 2013, (33) Perugini et al. 2008, (34) Tan et al. 2018, (35) Zou et al. 2018, (36) Ben-David et al. 2010, (37) Ji et al. 2008, (38) Yao et al. 2007, (39) Singrün et al. 2004, (40) Worthington et al. 2014, (41) Qiu et al. 2005, (42) Chhuneja et al. 2015, (43) Ouyang et al. 2014, (44) Han et al. 2009, (45) Luo et al. 2009, (46) Xiao et al. 2013, (47) Huang et al. 2002, (48) Lutz et al. 1995, (49) Zeller et al. 2002

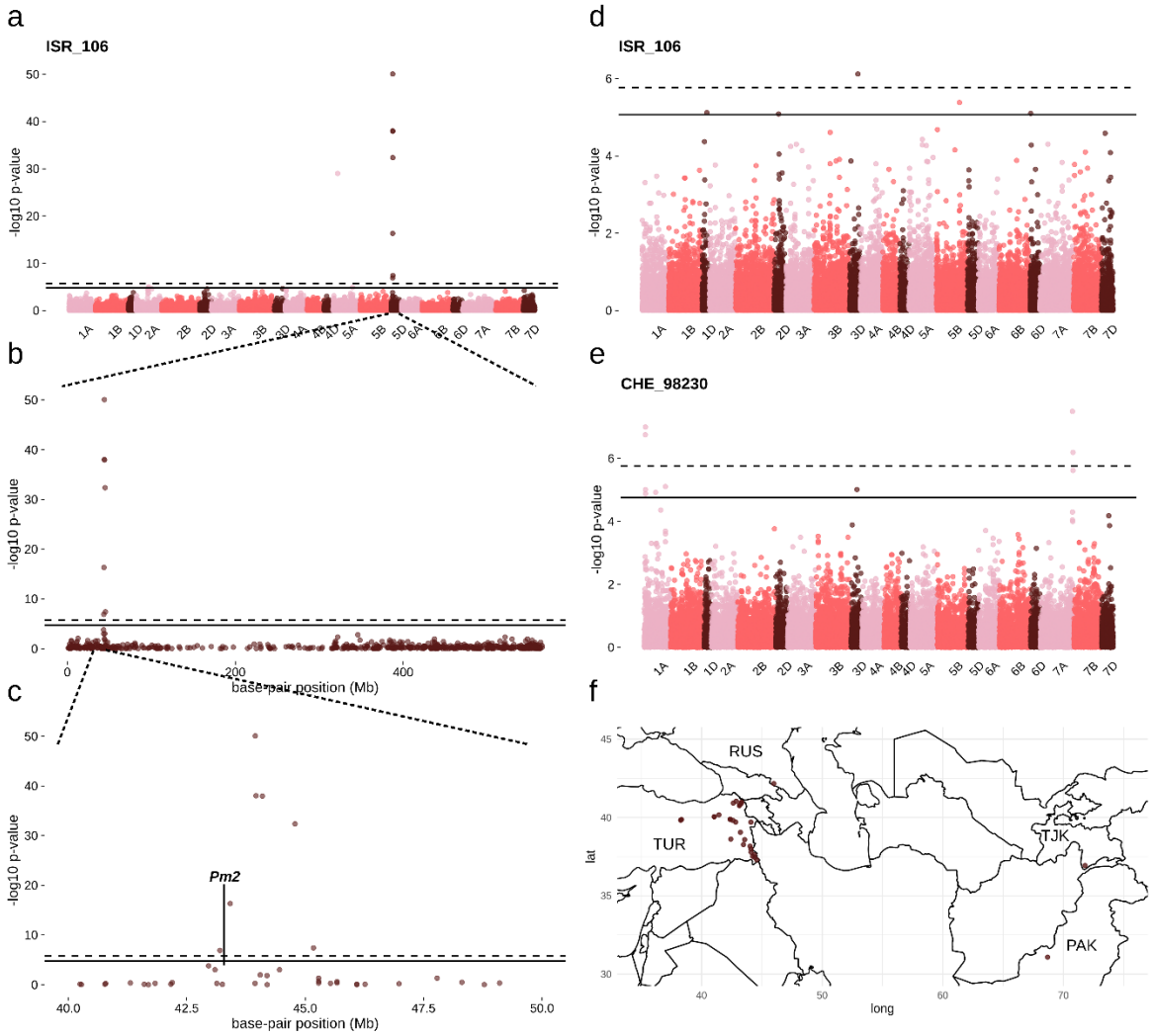

Figure 4. Analysis of the region associated with powdery mildew resistance on chromosome 5D

Manhattan plot for GWAS with all wheat accessions infected with isolate ISR_106 showing **a** all 21 chromosomes, **b** chromosome 5D and **c** the region of 40 to 50 Mb on chromosome 5D. The locus of the Chinese Spring version of *Pm2* with a partially deleted gene (Sánchez-Martín et al. 2016) is indicated with a line. **d** Manhattan plot for GWAS with

479 ISR_106 when adding a covariate for *Pm2* presence in wheat accessions. **e** Manhattan plot for the *Pm2* virulent
480 isolate CHE_98230. Solid lines represent the threshold for False discovery rate, and dashed lines for Bonferroni
481 correction. **f** Map with semitransparent brown dots depicting the origin of landraces that contain *Pm2*. Countries of
482 origin are abbreviated with the three-letter country code of ISO 3166

483

484 In addition to *Pm2*, we detected a peak on chromosome 1AS for CHE_98230, which spanned the genomic
485 region from 306,708 to 12,377,308 bp (Table 1, Fig S6) and contains the locus of the cloned gene *Pm3*.
486 Earlier studies have shown that out of 89 resistant accessions in the LandracePLUS panel, 21 contained
487 functional *Pm3* alleles, with twelve and five accessions containing *Pm3c* and *Pm3b*, respectively (Table S1)
488 (Bhullar et al. 2009, 2010a, 2010b). Therefore, we propose that the peak is caused by these functional
489 *Pm3* alleles.

490 A third, very large region on chromosome 2BL significantly showed CHE_96224 resistance-associated SNPs
491 from 707,987,645 to 722,628,991 bp (Table 1, Fig S6). Based on our criteria, this region was defined as
492 three independent peaks. Upon closer inspection, the peaks are, however, only separated by small
493 intervals showing no association. We therefore decided to consider them a single mildew-associated
494 region. Indeed, it was shown that an introgression on chromosome 2BL is present in the wheat gene pool,
495 most likely derived from the diploid wild relative *Triticum timopheevii* (Walkowiak et al. 2020; Keilwagen
496 et al. 2022). This introgression is potentially present in the LandracePLUS panel. Many candidate *Pm* genes
497 have already been described in this genomic interval, including *Pm51* (Zhan et al. 2014), *Pm63* (Tan et al.
498 2019), *PmKN0816* (Wang et al. 2021), *PmLS5082* (Wu et al. 2022), *PmQ* (Li et al. 2020b), *pmYN99102* (Mu
499 et al. 2022) and *PmCG15-009* (Zhang et al. 2023).

500 We further detected a peak on chromosome 7AL for CHE_94202, CHE_97266, CHE_98230 and GBR_JIW2
501 that spanned from 717,179,300 to 733,267,996 bp (Table 1, Fig S6). Possible candidate genes in this
502 genomic interval include *Pm59* (Tan et al. 2018), *Mlw72* (Ji et al. 2008), *Mlm2033* (Yao et al. 2007), *Mlm80*

503 (Yao et al. 2007), *MlUM15* (Worthington et al. 2014), *Mllw172* (Ouyang et al. 2014), *PmG16* (Ben-David
504 et al. 2010) and *mlRd30* (Singrün et al. 2004). Alleles of *Pm1* have also been mapped to chromosome 7AL
505 (McIntosh et al. 2013). However, we could not confirm an overlap with our resistance-associated region
506 because the *Pm1* locus is absent in Chinese Spring (IWGSC 2018).

507 Finally, we detected a peak on chromosome 7DL for GBR_JIW2 that spanned from 631,068,212 to
508 637,123,812 bp (Table 1, Fig S6, Fig 5a), where no *Pm* gene has been described previously.

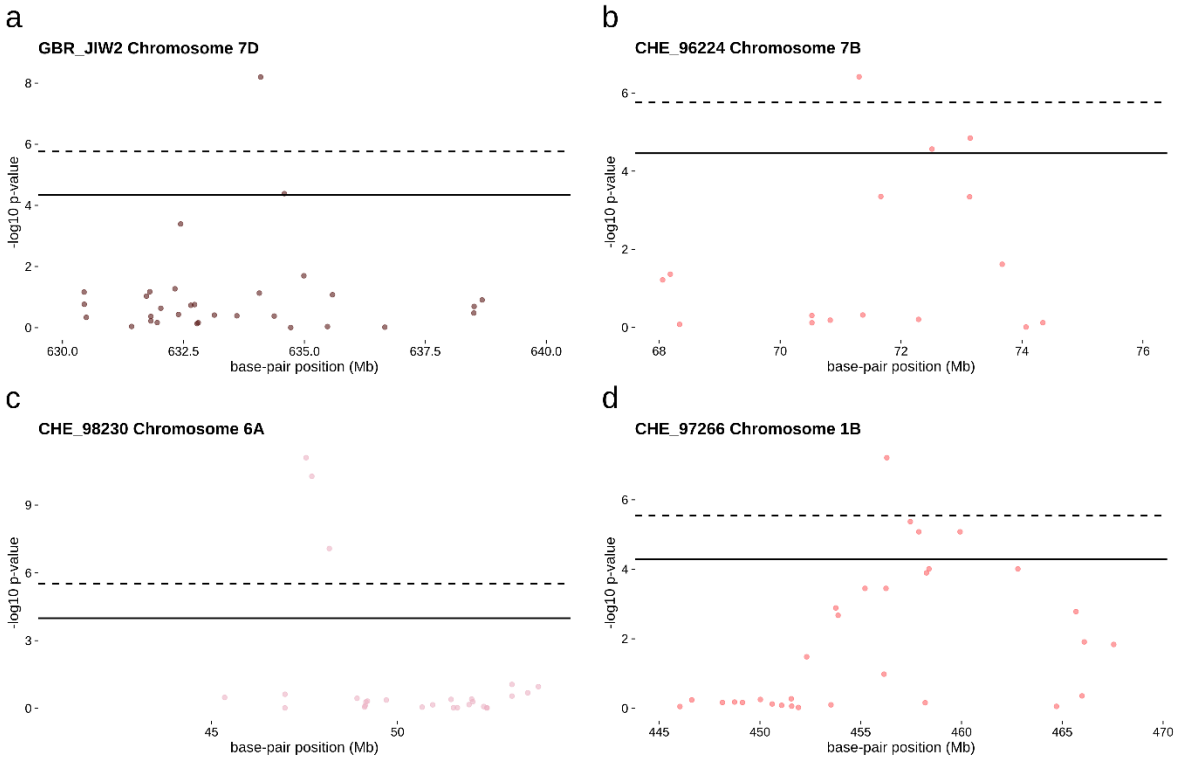

509

510 **Figure 5. Manhattan plots of novel resistance associated regions**

511 **a** All phenotyped LandracePLUS panel accessions. **b** All phenotyped LandracePLUS panel accessions using a *Pm2*
512 covariate. **c** Subset of accessions from Pakistan and Iran. **d** Subset of accessions from Turkey with CHE_97266
513 representing the peak occurring for multiple isolates. Isolates and chromosomes are depicted in the top-left corner.
514 Solid lines represent the threshold for False discovery rate and dashed lines for Bonferroni correction

515

516 Association studies with a *Pm2* covariate reveal five additional and novel resistance-associated loci

517 We used the information on the presence of *Pm2* in LandracePLUS panel accessions to detect further
518 resistance associations masked by the *Pm2* gene. Incorporating the covariate in GWAS for isolates with
519 the *Pm2* peak, we detected five additional associations on chromosomes 1B, 3B, 5B and 7B (Table 1, Fig
520 S7, Fig 5b). Two of these peaks appeared for CHE_96224, on chromosome 1BL, spanning from 610,940,301
521 to 615,710,501 bp and on chromosome 7BS from 68,921,370 to 73,691,570 bp. CHE_97266 showed an
522 association on chromosome 3BL from 701,911,458 to 706,681,658 bp and the last two associations
523 belonged to CHN_46_30, with a peak on chromosome 3BL from 667,372,099 to 672,142,299 bp and
524 another on chromosome 5BL from 647,102,735 to 651,872,935 bp. These associations occur in regions
525 where no *Pm* gene has been reported earlier, highlighting the utility of using a known *Pm* gene as a
526 covariate to discover new resistance loci in GWAS.

527 *Pm4* alleles are widely present in the LandracePLUS panel but are not revealed by association studies

528 Based on the resistance of differential lines carrying genes *Pm4a* or *Pm4b* to five and four of the nine
529 isolates, respectively (Sánchez-Martín et al. 2021), we expected to detect the cloned gene *Pm4* in the
530 LandracePLUS panel. Haplotype-specific markers detected the presence of the *Pm4* haplotype in 62
531 accessions. However, no peak was produced at the *Pm4* locus on chromosome 2AL for any isolate. To
532 explain this missing association despite the broad presence of *Pm4*, we sequenced the locus in all 62
533 accessions, of which 51 and four accessions contained the non-functional alleles *Pm4f* and *Pm4g*,
534 respectively (Sánchez-Martín et al. 2021; x), and four accessions with an undescribed allele, hereafter
535 *Pm4_42460*, while the functional alleles *Pm4b* and *Pm4d* only occurred once and twice, respectively. The
536 undescribed allele resembled *Pm4f*, except for one amino acid change in position 421 of splicing variant
537 V1 (L421P). While allele *Pm4g* was present in accessions of diverse geographical origin, 42 out of 51

538 accessions carrying *Pm4f* and all four accessions containing *Pm4_42460* were Turkish landraces. Our
539 findings suggest that the non-functional alleles *Pm4_42460* and *Pm4f* originated in Turkey.

540 Taken together, we find the presence of known *Pm* genes with GWAS of the LandracePLUS panel, giving
541 insights into their geographic distribution and potential origin. In addition, we discovered six genomic
542 regions where no *Pm* gene had been described earlier.

543 Utilizing subsets of the LandracePLUS panel discovers novel loci that are associated with powdery mildew
544 resistance of distinct geographical origin

545 Some resistance genes are likely present only in certain groups of the LandracePLUS panel, e.g., accessions
546 with similar geographical origins like for the *Pm2* resistance gene. Accordingly, we first tested if subsets
547 of the panel based on such groups were suitable to detect additional genomic regions associated with
548 powdery mildew resistance. To assess the sensitivity of this approach, we used a re-sampling approach
549 by creating 100 random subsets of 300, 200, 150 and 90 accessions from the LandracePLUS panel as input
550 for GWAS with the *Pm2* avirulent isolate ISR_106. Since the MAF threshold of 1% used above would not
551 filter out SNPs that occur only twice for a subset of 200 to 299 accessions, we adjusted the MAF threshold
552 to 5% for all subsets below a sample size of 300. We found the *Pm2*-associated peak in 100%, 87%, 78%
553 and 52% of cases for the four subset sizes, respectively. Therefore, we considered subsets of a minimum
554 of 150 to 200 accessions suitable for detecting loci associated with a major resistance gene in the
555 LandracePLUS panel.

556 In our sub-setting approach, we created sets of accessions based on their geographical origins. A subset
557 of landraces from Pakistan and Iran showed a good fit to the GWAS model only for the mildew isolate
558 CHE_98230 (Fig S8), revealing five additional peaks compared to the full LandracePLUS panel, located on
559 chromosomes 2B, 5A, 5B, 5D and 6A (Table 2, Fig S9, Fig 5c). While the peak on chromosome 2BL was
560 located in a genomic region that has been described to contain the resistance gene *Pm51* (Zhan et al.

561 2014) and the peak on chromosome 5BL has been implicated earlier with the resistance genes *Pm53*
562 (Petersen et al. 2015) and *Ml3D232* (Zhang et al. 2010), the associated regions on chromosomes 5AL from
563 679,959,567 to 692,030,167 bp and on 5DS from 26,487,899 to 32,543,499 bp have not been associated
564 with powdery mildew resistance before to our knowledge (Table 2). The last resistance-associated region,
565 on chromosome 6AS, spanned the region from 41,508,045 to 53,578,645 (Fig 5c). On chromosome arm
566 6AS, only *Pm21* and *Pm56* have been described. *Pm21* originated and was cloned from the diploid grass
567 *Dasypyrum villosum* (He et al. 2018; Xing et al. 2018). The gene was introduced in the hexaploid gene pool
568 in China through a translocation line T6AL.6VS in the late 1980s (Chen et al. 1995). However, the
569 translocated arm from *D. villosum* does not recombine with wheat homeologs (He et al. 2017). Hence, we
570 expect to see a broad association covering the short arm of chromosome 6A in the case of *Pm21* detection.
571 Further, *Pm21* was described to confer broad-spectrum resistance (He et al. 2017), whereas we observed
572 the association for only one out of ten isolates. Therefore, we assume that the causal gene in our
573 resistance-associated region differs from *Pm21*. Similarly, *Pm56* was only recently introduced as a
574 translocation line 6AL.6RS from rye (Hao et al. 2018) several years after we obtained and utilized the seeds
575 of the initial collection. We conclude that this is a resistance-associated region on chromosome 6AS not
576 previously described.

577 **Table 2. Powdery mildew associated regions detected in subsets of the LandracePLUS panel**

Chr	Position	Subset	Isolate	beta	*Pm* genes described on specific chromosome (arm)
1AL	539,831,968 – 551,902,568	Turkey (221)	CHE_98230	-0.14	*Pm25*(1)
1BL	453,908,676 – 462,314,398	Turkey (223, 222, 222, 217, 212)	CHE_94202 CHE_96224 CHE_97266 CHN_46_30 ISR_106	-0.22 -0.24 -0.26 -0.28 -0.26	*Pm28*(2), *Pm39*(3)
1BL	664,434,720 – 669,204,920	Turkey (222)	CHE_96224	-0.22	*Pm28*(2), ***Pm39***(3)

1DL	333,346,020 – 339,401,620	Turkey (217, 212)	CHN_46_30 ISR_106	-0.48 -0.48	*Pm10*(4)
2AL	534,734,122 – 546,804,722	Turkey (221)	CHE_98230	0.38	*Pm4*(5), *Pm50*(6), *Pm65*(7), *pmX*(8), *PmHo*(9), *Ml92145E8-9*(10), *PmHNK54*(11), *PmLK906*(12), *PmYm66*(13), *PmSN15218*(14)
2AL	762,574,656 – 774,645,256	Turkey (221)	CHE_98230	0.84	*Pm4*(5), *Pm50*(6), ***Pm65***(7), ***pmX***(8), *PmHo*(9), *Ml92145E8-9*(10), *PmHNK54*(11), *PmLK906*(12), *PmYm66*(13), ***PmSN15218***(14)
2BL	737,551,805 – 742,322,005	Pakistan/Iran (167)	CHE_98230	-0.33	*Pm6*(15), *Pm33*(16), ***Pm51***(17), *Pm52*(18), *Pm57*(19), *Pm62 (20)*, *Pm63*(21), *Pm64*(22), *PmKN0816*(23), *PmLS5082*(24), *PmQ*(25), *PmY39*(26), *pmYN99102*(27), *MlAB10*(28), *Mlzec1*(29), *PMCG15-009*(30)
3AL	643,922,092 – 655,992,692	Turkey (220)	GBR_JIW2	-0.16	-
4BL	610,988,411 – 615,758,611	Turkey (224)	CHE_97223	-0.12	*Pm7*(31), *Mld*(32), *PmTx45*(33)
5AL	472,287,696 – 484,857,509	Turkey (217)	CHN_46_30	0.16	*pm2026*(34)
5AL	679,959,567 – 692,030,167	Pakistan/Iran (167)	CHE_98230	0.28	*pm2026*(34)
5BL	375,685,467 – 380,455,667	Turkey (223)	CHE_94202	-0.20	*Pm36*(35), *Pm53*(36), *PmAS846*(37), *Ml3D232*(38)
5BL	517,686,966 – 522,457,166	Pakistan/Iran (167)	CHE_98230	0.19	*Pm36*(35), ***Pm53***(36), *PmAS846*(37), ***Ml3D232***(38)
5BL	656,831,925 – 661,602,125	Turkey (217)	CHN_46_30	0.19	*Pm36*(35), *Pm53*(36), *PmAS846*(37), *Ml3D232*(38)
5DS	26,487,899 – 32,543,499	Pakistan/Iran (167)	CHE_98230	0.27	*Pm2*(39), *Pm46* (40), *Pm55*(41)
6AS	0 – 7,996,136	Turkey (224)	CHE_97223	-0.12	*Pm21*(42, 43), *Pm56*(44)
6AS	41,508,045 – 53,578,645	Pakistan/Iran (167)	CHE_98230	-0.25	*Pm21*(42, 43), *Pm56*(44)
7AL	611,542,221 – 623,612,821	Turkey (224)	CHE_97223	-0.09	*Pm1*(45), *Pm9* (46), *Pm37*(47), *Pm59(48)*, *Pm60*(49), *PmG16*(50), *MlIw72*(51), *Mlm2033*(52), *Mlm80*(52), *mlRd30*(53), *MlUM15*(54), *PmU*(55), *PmTb7A.1*(56), *PmTb7A.2*(56), *MlIW172*(57), *MlWE18*(58)

7BL	701,729,427 – 706,653,524	Turkey (221)	CHE_98230	-0.16	***Pm5***(59)*,* ***pmDHT***(60)*,* ***PmSGD***(61)*,* ***PmTm4***(62)*,* ***pmHYM***(63)*,* ***pmYBL***(64)*,* ***mlxbd***(65)*,* *mljy*(66)*,* *mlsy*(66)
7DL	497,931,007 – 503,986,607	Turkey (223, 222, 217, 212)	CHE_94202 CHE_96224 CHN_46_30 ISR_106	-0.16 -0.15 -0.16 -0.19	*Pm19*(67), *Pm29*(68)

578 Physical positions of GWAS peaks on Chinese Spring, subset description with number of accessions in brackets and
579 the isolates detecting them. Chr = chromosome. Values for beta are shown for the SNP of each peak with the
580 strongest effect size. If several isolates produce the same peak, beta is listed for each. *Pm* genes are listed that were
581 described on the same chromosomal arm or the same chromosome without a specified arm. *Pm* genes described in
582 an overlapping genomic interval with the GWAS peak are highlighted in bold. (1) Shi et al. 1998, (2) Peusha et al.
583 2004, (3) Lillemo et al. 2008, (4) Tosa et al. 1987, (5) Sánchez-Martín et al. 2021, (6) Mohler et al. 2013, (7) Li et al.
584 2019, (8) Fu et al. 2013, (9) Komáromi et al. 2016, (10) Yu et al. 2018, (11) Xu et al. 2011, (12) Niu et al. 2008, (13) Hu
585 et al. 2008, (14) Sun et al. 2022, (15) Wan et al. 2020, (16) Zhu et al. 2005, (17) Zhan et al. 2014, (18) Wu et al. 2019,
586 (19) Dong et al. 2020, (20) Zhang et al. 2018, (21) Tan et al. 2019, (22) Zhang et al. 2019, (23) Wang et al. 2021, (24)
587 Wu et al. 2022, (25) Li et al. 2020, (26) Zhu et al. 2006, (27) Mu et al. 2022, (28) Maxwell et al. 2010, (29) Mohler et
588 al. 2005, (30) Zhang et al. 2023, (31) Driscoll and Bielig 1968, (32) McIntosh et al. 2013, (33) Chao et al. 2019, (34) Xu
589 et al. 2008, (35) Blanco et al. 2008,(36) Petersen et al. 2015, (37) Xue et al. 2012, (38) Zhang et al. 2010, (39) Sánchez-
590 Martín et al. 2016, (40) Gao et al. 2012, (41) Zhang et al. 2016, (42) He et al. 2018, (43) Xing et al. 2018, (44) Hao et
591 al. 2018, (45) Hewitt et al. 2021, (46) McIntosh et al. 2013, (47) Perugini et al. 2008, (48) Tan et al. 2018, (49) Zou et
592 al. 2018, (50) Ben-David et al. 2010, (51) Ji et al. 2008, (52) Yao et al. 2007, (53) Singrün et al. 2004, (54) Worthington
593 et al. 2014, (55) Qiu et al. 2005, (56) Chhuneja et al. 2015, (57) Ouyang et al. 2014, (58) Han et al. 2009, (59) Hsam
594 et al. 2001, (60) Qie et al. 2019, (61) Xu et al. 2018, (62) Xie et al. 2017, (63) Wang et al. 2022, (64) Xu et al. 2020,
595 (65) Jin et al. 2020, (66) Huang et al. 2002, (67) Lutz et al. 1995, (68) Zeller et al. 2002

596

597 Finally, we used the same geographical approach to investigate only Turkish landraces, revealing a good
598 fit to the model for all isolates except CHE_19004 (Fig S10). This subsetting resulted in the discovery of 15
599 additional peaks on chromosomes 1A, 1B, 1D, 2A, 3A, 4B, 5A, 5B, 6A, 7A, 7B and 7D (Table 2, Fig S11). In
600 earlier studies, two of the 15 regions have been described with powdery mildew seedling resistance. The
601 associated region on chromosome 2AL from 762,574,656 to 774,645,256 bp covers three known *Pm*
602 genes, while the peak on chromosome 7BL from 701,729,427 to 706,653,524 bp overlaps with eight

603 previously described *Pm* genes (Table 2). The association on chromosome 1BL from 664,434,720 to
604 669,204,920 bp includes the *Pm39* locus. However, *Pm39*, also known as *Lr46* (Lillemo et al. 2008), is an
605 adult plant resistance gene and not active at seedling stage, and we conclude that the detected
606 association is caused by an unknown, novel gene. The remaining twelve loci do not overlap with previously
607 described *Pm* genes and therefore depict good candidates for novel powdery mildew resistance loci (Table
608 2).

609 Taken together, subsets based on geographical origin revealed 16 genomic regions where no *Pm* genes
610 have been described previously, suggesting that these genes arose in the respective countries Pakistan,
611 India and Turkey.

612 <u>Candidate genes of five novel resistance loci include putative NLRs, serine/threonine kinases, a C2H2-type</u>
613 <u>zinc finger and F-box-like proteins with leucine-rich repeat (LRR) domains</u>

614 We investigated five of the 22 novel resistance loci more closely to get an insight into possible candidate
615 genes (Figure 5, Table S6). We chose the most significant peak with at least two significantly associated
616 SNPs from GWAS of 1) the full LandracePLUS panel, 2) the panel using the *Pm2* covariate and 3) the
617 Pakistan/Iran subset, on chromosomes 7DL, 7BS and 6AS, respectively. From the subset of Turkish
618 landraces, we chose the highly significant single SNP association on chromosome 1DL and the peak on
619 chromosome 1BL that occurred for five isolates, suggesting a more broad-spectrum resistance. For the
620 associated region on chromosome 7DL, candidates annotated on Chinese Spring were ten putative NLRs,
621 while the associated region on chromosome 7BS contained an annotation for a C2H2-type zinc finger and
622 one F-box-like protein with an LRR domain. All associated regions except for 1BL had annotations for one
623 serine/threonine kinase, the only candidate for the peak on chromosome 1DL. Both peaks on
624 chromosome 6AS and 1BL each contained annotations for one putative NLR and the peak on chromosome

625 6AS included four additional F-box-like proteins with LRR domains (Figure 5, Table 6). Further validation
626 studies are necessary to confirm the resistant nature of these candidate genes.

627 Novel resistance loci for breeding programs

628 We analyzed the gene pool of the twenty most modern cultivars of the LandracePLUS panel (registered
629 between 1990 and 2003) to evaluate whether the 22 potentially novel powdery mildew genes are present
630 in elite material or potentially novel in this gene pool (Supplementary_file3). For genomic regions on
631 chromosomes 5BL (derived from the LandracePLUS panel using a *Pm2* covariate) and 6AS (from the
632 Pakistan/Iran subset), the most modern cultivars contained less than 50% of the resistance-associated
633 SNPs, suggesting that the underlying resistance genes are likely not present in these cultivars. For six of
634 the 22 associations, including the peaks on chromosomes 7DL and 1BL (described above in detail), some
635 of the cultivars contained at least 50% of the resistance-associated SNPs, but none showed resistance
636 towards the respective mildew isolate. We conclude that the underlying resistance genes are not present
637 in this germplasm, at least not as active, resistance-conferring alleles. These findings suggest that the
638 resistance loci have not been transferred to the modern gene pool from landraces. However, investigation
639 of more recent cultivars would be needed to confirm these results.

640 Resistance-associated SNPs of the remaining 14 associated regions, including the peaks on chromosomes
641 7BS and 1DL discussed extensively, were present in the most modern germplasm. However, few
642 accessions that harbored the alleles were resistant. Thus, the underlying resistance-conferring alleles
643 seem to be partially present, meaning that breeders could integrate the corresponding cultivars we
644 highlighted (Supplementary_file3) directly in their programs, avoiding possible yield penalties due to
645 linkage drag. However, the combination of resistance and presence of resistance-associated SNPs
646 occurred only for the three cultivars TRI 17181, TRI 17284 and TRI 16947. While these cultivars are

647 attractive resistance-breeding candidates, it is difficult to dissect which detected regions are causing the
648 observed resistance and, therefore, actually contain causative alleles.

649

650 **Discussion**

651 The LandracePLUS panel harbors untapped genetic diversity originating mainly from Turkish, Pakistani
652 and Iranian landraces

653 We assembled a diverse panel of 755 bread wheat accessions with a focus on landraces. A FIGS approach
654 laid the foundation for a trait-customized collection of accessions with potentially high selection pressure
655 for powdery mildew resistance. A second step of selective reduction based on geographical origin resulted
656 in the LandracePLUS panel. Mantel tests revealed a small impact of the population structure on powdery
657 mildew resistance variation, reflecting the successful outcome of our targeted panel assembly. The
658 resulting improved power of GWAS (Myles et al. 2009) facilitated the detection of novel *Pm* genes in the
659 LandracePLUS panel.

660 The LandracePLUS panel revealed untapped genetic diversity in Turkish, Iranian and Pakistani landraces.
661 It showed four main genetic clusters that correlate with the geographical origin, similar to a study which
662 showed that wheat accessions from the Caucasus region, as well as Central, South and East Asian are more
663 diverse compared to other regions in the world (Balfourier et al. 2019). Landraces covered almost the full
664 diversity of the LandracePLUS panel, whereas cultivars were limited to one cluster. This cluster also
665 included the bread wheat accessions with high-quality sequenced genomes, except for the two landraces
666 Chinese Spring and Norin61 (IWGSC et al. 2018; Walkowiak et al. 2020; Sato et al. 2021; Aury et al. 2022).
667 This observation highlights the need to include landraces in breeding programs to enlarge the genetic
668 base of elite wheat varieties (Lopes et al. 2015; Marone et al. 2021). Future diversity studies of wheat

669 should focus on landraces, in particular on those from regions with untapped genetic diversity, such as
670 Turkey, Pakistan and Iran.

671 Pathogen virulence characterization guides *Pm* gene discovery

672 To discover novel *R* genes against powdery mildew in the LandracePLUS panel, we used a set of ten *Bgt*
673 isolates that showed highly diverse virulence patterns when tested on differential lines with single, known
674 *Pm* genes. As we observed avirulence for many differential lines, using these isolates should reveal the
675 presence of most *Pm* genes for which differential lines are available.

676 The tested wheat accessions were rarely resistant to more than three isolates, in line with characteristic
677 *R* gene-based race-specific resistance (Flor 1971). This implies that the observed single resistance genes
678 would be of limited agricultural use, depending on the isolates present in the corresponding wheat-
679 growing area. To broaden the resistance spectrum and prevent fast evolution of pathogen virulence, such
680 genes should be deployed in a suitable manner, e.g., by gene stacking, gene pyramiding or transgenic
681 overexpression (Mundt 2018; Koller et al. 2019). On the other hand, the accessions of the LandracePLUS
682 panel susceptible to all tested powdery mildew isolates can be assumed to lack any major resistance gene
683 active at the seedling stage. Thus, observed resistance in adult plants in the field would likely be durable,
684 making such accessions attractive donors of adult plant resistance.

685 Currently, for the 27 genes represented in the differential set of *Pm* lines used in this study, only eight of
686 the corresponding avirulence genes are molecularly known (Bourras et al. 2015, 2019; Praz et al. 2017;
687 Hewitt et al. 2021; Müller et al. 2022; Kloppe et al. 2023; Kunz et al. 2023). Avirulence gene sequence
688 comparison in our ten powdery mildew isolates revealed the presence of recognized haplotypes of seven
689 of the cloned Avrs. This knowledge guided us to determine whether a resistance-associated region in the
690 LandracePLUS panel was derived from a known *Pm* gene, as we showed for the cloned gene *Pm2a*.
691 Further, the information on resistance to *Bgt* isolates of distinct geographical origin can guide an informed

692 deployment of accessions in the respective agricultural areas (Vleeshouwers and Oliver 2014; Müller et
693 al. 2022). For example, our findings suggest further work on landraces resistant to CHN_46_30 for
694 potential deployment in China because they must contain effective *R* genes against this isolate of Chinese
695 origin.

696 GWAS of the LandracePLUS panel detects known *Pm* genes and reveals six undescribed powdery mildew
697 resistance-associated regions on chromosomes 1BL, 3BL, 5BL, 7BS and 7DL

698 GWAS for eight powdery mildew isolates on the LandracePLUS panel without subsetting revealed ten
699 resistance-associated regions. Four of these were in genomic regions with previously described resistance
700 genes. Of these, the peaks on chromosomes 2BL and 7AL overlapped with regions of genetically described,
701 but not molecularly known *Pm* genes, while the peaks on chromosomes 1AS and 5DS were likely caused
702 by the cloned genes *Pm3* and *Pm2*, respectively. While *Pm3* was known to be present in several
703 LandracePLUS panel accessions (Bhullar et al. 2009, 2010a, 2010b), we did not expect to find *Pm2* widely
704 in the gene pool of landraces. *Pm2* was introduced into the breeding gene pool via the Russian cultivar
705 Ulka (Pugsley and Carter 1953). It originated from the diploid wheat wild relative *Ae. tauschii* and has eight
706 known haplotypes, of which only *Pm2a* was detected in hexaploid wheat (Manser et al. 2021). While *Pm2a*
707 has been identified previously in six wheat landraces (Chen et al. 2019; Manser et al. 2021), we found its
708 presence in 34, mostly Turkish landraces, suggesting Turkey as the geographical origin of the *Pm2a*
709 resistance gene. While GWAS did not detect the cloned gene *Pm4* in the LandracePLUS panel, we
710 discovered a high frequency of two non-functional *Pm4* alleles in Turkish landraces. Our findings suggest
711 that these alleles originated in Turkey, fitting the origin of *Pm4* from tetraploid wheat, which also arose in
712 Turkey (Özkan et al. 2002; Sánchez-Martín et al. 2021). Despite the narrow representation of *Pm4b* and
713 *Pm4d* in landraces, a wide presence of these functional alleles compared to *Pm4f* and *Pm4g* has been
714 described in elite germplasm (Sánchez-Martín et al. 2021). This suggests that the breeding process for
715 *Pm4* mildew resistance was very effective.

716 We detected one region on chromosome 7DL not previously described as associated with mildew
717 resistance. This region contained annotations for ten putative NLRs and one serine/threonine kinase.
718 While NLRs are to date still the most common candidates for *Pm* genes, serine/threonine kinases have
719 been described to play a role in defense response, including *Pto*, which confers resistance to bacterial
720 speck disease in tomato (Martin et al. 1993; Loh and Martin 1995).

721 Using a *Pm2* covariate, we detected five additional undescribed resistance associations in the
722 LandracePLUS panel. One of them was located on chromosome 7BS, containing candidate genes
723 putatively encoding a C2H2-type Zinc finger, a serine/threonine kinase and an F-box-like protein with LRR
724 domains. The latter have been described to facilitate hypersensitive cell death response in tobacco and
725 tomato (Van Den Burg et al. 2008) and shown to be involved in defense response to stripe rust in wheat
726 (Yin et al. 2018). On the other hand, Zinc fingers of the C2H2-type were linked to plant defense response
727 (Kim et al. 2004; Tian et al. 2010; Yin et al. 2020; Sharma et al. 2021), where some cases have shown that
728 the transcriptional repression activity of the zinc finger was the mechanism behind this association
729 (Weigel et al. 2005; Uehara et al. 2005).

730 Targeted GWAS subsets reveal 16 potentially novel resistance-associated loci

731 Utilizing targeted subsets, we discovered 16 most likely novel peaks on ten chromosomes (Table 2). GWAS
732 are expected to be more powerful when conducted on large datasets where individuals are drawn
733 randomly from the population (Uffelmann et al. 2021). However, important SNPs at a small regional scale
734 might yet be diluted in species-wide panels and not detected by GWAS, which typically lacks the power
735 to detect associations with rare alleles (Marees et al. 2018). Pending sufficient phenotypic and genetic
736 variation, GWAS in local panels have proven very effective in *Arabidopsis thaliana* (Gloss et al. 2022). For
737 this reason, resistance genes which may have been selected at small regional scales might be more
738 efficiently detected in subsets of accessions from the same geographical origin.

739 Therefore, we focused on accessions originating from distinct countries that harbored novel genetic
740 diversity, namely Pakistan, Iran and Turkey. This resulted in the detection of 16 additional loci where no
741 *Pm* genes have been described. With a subset of accessions exclusively from Pakistan or Iran, we
742 discovered a region on chromosome 6AS associated with mildew resistance. The region contains genes
743 putatively encoding an NLR, a serine/threonine kinase and F-box-like proteins with LRR domains.

744 While we present novel regions and gene candidates, the molecular nature of the observed resistance
745 must be confirmed in future studies, especially when considering that the reference genome Chinese
746 Spring might lack (susceptible) alleles of the causal resistance genes. One approach would be the
747 application of recent sequencing technologies, such as circular consensus sequencing (CCS) (Wenger et al.
748 2019). Such novel approaches have increased the feasibility of sequencing single donor accessions to
749 assist in the cloning a gene of interest. For example, assembling the Kariega genome with CCS has
750 demonstrated the usefulness of this approach in wheat and has led to the cloning of *Yr27* (Athiyannan et
751 al. 2022a). Another option to identify a gene of interest in a specific genotype depends on the availability
752 of a pangenome, which ideally would capture the entire gene repertoire of a species (Tettelin et al. 2005).
753 High-quality sequencing efforts have recently resulted in 19 wheat genomes, of which 14 have reference
754 genome quality (IWGSC et al. 2018; Walkowiak et al. 2020; Sato et al. 2021; Aury et al. 2022; Athiyannan
755 et al. 2022a; Kale et al. 2022). Genome analysis has revealed structural rearrangements, introgressions
756 and differences in gene content (Walkowiak et al. 2020). A successful example of using this resource is
757 the cloning of *Lr14a*, which was based on the reference genome ArinaLrFor (Kolodziej et al. 2021).
758 However, despite the recent advances in pangenome projects, the close clustering of the high-quality
759 sequenced genomes compared to the LandracePLUS panel suggests that the currently available
760 pangenome includes only a fraction of the diversity present in landraces, including resistance loci. Thus,
761 it is essential to include more diverse wheat accessions, specifically landraces, in future work to increase
762 the extent of the pangenome, particularly for NLR loci, which are rarely present across wheat genotypes.

763 We propose to assemble high-quality genomes of several landraces from Turkey, Pakistan and Iran to
764 achieve such a goal. Furthermore, contrasting phenotypes for traits of interest should be included when
765 setting up pangenome consortia. This diversified selection could provide a resource that guides various
766 trait-genotype associations. Finally, we suggest choosing a donor accession with confirmed resistance for
767 each peak and sequencing the resistance-associated genome using CCS. This will reveal which gene
768 candidates are present in the specific accessions and guide their molecular cloning and validation, e.g.,
769 via virus-induced gene silencing (Cakir et al. 2010).

770 The subset-based association analysis done in this work of the genetically diverse LandracePLUS panel
771 challenged with ten *Bgt* isolates unraveled 22 potentially novel powdery mildew resistance genes.
772 Therefore, this study can be used as an example for future work on similar collections in search of other
773 traits of interest. Once a diversity panel is assembled, instead of focusing on single pathogen races,
774 phenotyping with diverse isolates from geographically defined agricultural regions followed by subset-
775 based analyses for the origin of accessions, would reveal more resistance loci compared to studies done
776 with single pathogen isolates on entire collections.

777

778 **References**

779 Alemu SK, Huluka AB, Tesfaye K, et al (2021) Genome-wide association mapping identifies
780 yellow rust resistance loci in Ethiopian durum wheat germplasm. PLoS One
781 16:e0243675. https://doi.org/10.1371/journal.pone.0243675

782 Alexander DH, Novembre J, Lange K (2009) Fast model-based estimation of ancestry in
783 unrelated individuals. Genome Res 19:1655–1664.
784 https://doi.org/10.1101/gr.094052.109

785 Athiyannan N, Abrouk M, Boshoff WHP, et al (2022a) Long-read genome sequencing of
786 bread wheat facilitates disease resistance gene cloning. Nat Genet 54:227–231.
787 https://doi.org/10.1038/s41588-022-01022-1

788 Athiyannan N, Aouini L, Wang Y, Krattinger SG (2022b) Unconventional R proteins in the
789 botanical tribe Triticeae. Essays Biochem 66:561–569.
790 https://doi.org/10.1042/EBC20210081

791 Aury JM, Engelen S, Istace B, et al (2022) Long-read and chromosome-scale assembly of the
792 hexaploid wheat genome achieves high resolution for research and breeding.
793 Gigascience 11:1–18. https://doi.org/10.1093/gigascience/giac034

794 Balfourier F, Bouchet S, Robert S, et al (2019) Worldwide phylogeography and history of
795 wheat genetic diversity. Sci Adv 5:. https://doi.org/10.1126/sciadv.aav0536

796 Bates D, Mächler M, Bolker BM, Walker SC (2015) Fitting linear mixed-effects models using
797 lme4. J Stat Softw 67:1–48. https://doi.org/10.18637/jss.v067.i01

798 Ben-David R, Xie W, Peleg Z, et al (2010) Identification and mapping of PmG16, a powdery
799 mildew resistance gene derived from wild emmer wheat. Theoretical and Applied
800 Genetics 121:499–510. https://doi.org/10.1007/s00122-010-1326-5

801 Bhullar NK, Mackay M, Keller B (2010a) Genetic Diversity of the Pm3 Powdery Mildew
802 Resistance Alleles in Wheat Gene Bank Accessions as Assessed by Molecular Markers.
803 Diversity (Basel) 2:768–786. https://doi.org/10.3390/d2050768

804 Bhullar NK, Street K, Mackay M, et al (2009) Unlocking wheat genetic resources for the
805 molecular identification of previously undescribed functional alleles at the Pm3
806 resistance locus. Proc Natl Acad Sci U S A 106:9519–9524.
807 https://doi.org/10.1073/pnas.0904152106

808 Bhullar NK, Zhang Z, Wicker T, Keller B (2010b) Wheat gene bank accessions as a source of
809 new alleles of the powdery mildew resistance gene Pm3: A large scale allele mining
810 project. BMC Plant Biol 10:88. https://doi.org/10.1186/1471-2229-10-88

811 Blanco A, Gadaleta A, Cenci A, et al (2008) Molecular mapping of the novel powdery mildew
812 resistance gene Pm36 introgressed from Triticum turgidum var. dicoccoides in durum
813 wheat. Theoretical and Applied Genetics 117:135–142.
814 https://doi.org/10.1007/s00122-008-0760-0

815 Bonjean AP, Angus WJ (2001) The world wheat book: a history of wheat breeding. Lavoisier
816 Publishing Inc.

817 Bourguet D, Guillemaud T (2016) The Hidden and External Costs of Pesticide Use. Springer,
818 Cham, pp 35–120

819 Bourras S, Kunz L, Xue M, et al (2019) The AvrPm3-Pm3 effector-NLR interactions control
820 both race-specific resistance and host-specificity of cereal mildews on wheat. Nat
821 Commun 10:1–16. https://doi.org/10.1038/s41467-019-10274-1

822 Bourras S, McNally KE, Ben-David R, et al (2015) Multiple Avirulence Loci and Allele-Specific
823 Effector Recognition Control the *Pm3* Race-Specific Resistance of Wheat to Powdery
824 Mildew. Plant Cell 27:tpc.15.00171. https://doi.org/10.1105/tpc.15.00171

825 Bradbury PJ, Zhang Z, Kroon DE, et al (2007) TASSEL: software for association mapping of
826 complex traits in diverse samples. Bioinformatics 23:2633–2635.
827 https://doi.org/10.1093/bioinformatics/btm308

828 Brown JKM (2015) Durable Resistance of Crops to Disease: A Darwinian Perspective. Annu
829 Rev Phytopathol 53:513–539. https://doi.org/10.1146/annurev-phyto-102313-045914

830 Browning BL, Zhou Y, Browning SR (2018) A One-Penny Imputed Genome from Next-
831 Generation Reference Panels. Am J Hum Genet 103:338–348.
832 https://doi.org/10.1016/j.ajhg.2018.07.015

833 Cakir C, Gillespie ME, Scofield SR (2010) Rapid Determination of Gene Function by Virus-
834 induced Gene Silencing in Wheat and Barley. Crop Sci 50:S-77-S-84.
835 https://doi.org/10.2135/cropsci2009.10.0567

836 CGIAR (2023) Genebank Platform. https://www.genebanks.org/resources/crops/wheat/.
837 Accessed 8 Mar 2023

838 Chao K, Su W, Wu L, et al (2019) Molecular Mapping of a Recessive Powdery Mildew
839 Resistance Gene in Wheat Cultivar Tian Xuan 45 Using Bulked Segregant Analysis with
840 Polymorphic Single Nucleotide Polymorphism Relative Ratio Distribution.
841 Phytopathology 109:828–838. https://doi.org/10.1094/PHYTO-03-18-0092-R

842 Chen F, Jia H, Zhang X, et al (2019) Positional cloning of PmCH1357 reveals the origin and
843 allelic variation of the Pm2 gene for powdery mildew resistance in wheat. Crop Journal
844 7:771–783. https://doi.org/10.1016/j.cj.2019.08.004

845 Chen PD, Qi LL, Zhou B, et al (1995) Development and molecular cytogenetic analysis of
846 wheat-Haynaldia villosa 6VS/6AL translocation lines specifying resistance to powdery
847 mildew. Theoretical and Applied Genetics 91:1125–1128.
848 https://doi.org/10.1007/BF00223930

849 Chhuneja P, Yadav B, Stirnweis D, et al (2015) Fine mapping of powdery mildew resistance
850 genes PmTb7A.1 and PmTb7A.2 in Triticum boeoticum (Boiss.) using the shotgun
851 sequence assembly of chromosome 7AL. Theoretical and Applied Genetics 128:2099–
852 2111. https://doi.org/10.1007/s00122-015-2570-5

853 Danecek P, Auton A, Abecasis G, et al (2011) The variant call format and VCFtools.
854 Bioinformatics 27:2156–2158. https://doi.org/10.1093/bioinformatics/btr330

855 de Vries A, Ripley BD (2022) Create Dendrograms and Tree Diagrams Using “ggplot2”

856 Dodds PN, Rathjen JP (2010) Plant immunity: Towards an integrated view of plant-pathogen
857 interactions. Nat Rev Genet 11:539–548. https://doi.org/10.1038/nrg2812

858 Dong Z, Tian X, Ma C, et al (2020) Physical Mapping of Pm57, a Powdery Mildew Resistance
859 Gene Derived from Aegilops searsii. Int J Mol Sci 21:322.
860 https://doi.org/10.3390/ijms21010322

Dormann CF, Schweiger O, Augenstein I, et al (2007) Effects of landscape structure and land-use intensity on similarity of plant and animal communities. Global Ecology and Biogeography 16:774–787. https://doi.org/10.1111/j.1466-8238.2007.00344.x

Dracatos PM, Lu J, Sánchez-Martín J, Wulff BBH (2023) Resistance that stacks up: engineering rust and mildew disease control in the cereal crops wheat and barley. Plant Biotechnol J 21:1938–1951. https://doi.org/10.1111/pbi.14106

Driscoll CJ, Bielig LM (1968) MAPPING OF THE TRANSEC WHEAT-RYE TRANSLOCATION. Canadian Journal of Genetics and Cytology 10:421–425. https://doi.org/10.1139/g68-056

EU 2020 Farm to Fork. https://ec.europa.eu/commission/presscorner/detail/en/qanda_22_3694. Accessed 8 Mar 2023

Evenson RE, Gollin D (2003) Assessing the impact of the Green Revolution, 1960 to 2000. Science (1979) 300:758–762. https://doi.org/10.1126/science.1078710

FAO (2020) Food and Agriculture Organization of the United Nations, FAOSTAT statistics database, Food Balances. https://www.fao.org/faostat/en/#data/FBS. Accessed 8 Mar 2023

Flor HH (1971) Current status of the gene-for-gene concept. Annu Rev Phytopathol 9:275–296

Fu B, Chen Y, Li N, et al (2013) pmX: A recessive powdery mildew resistance gene at the Pm4 locus identified in wheat landrace Xiaohongpi. Theoretical and Applied Genetics 126:913–921. https://doi.org/10.1007/s00122-012-2025-1

Galili T (2015) dendextend: an R package for visualizing, adjusting and comparing trees of hierarchical clustering. Bioinformatics 31:3718–3720. https://doi.org/10.1093/bioinformatics/btv428

Gao H, Zhu F, Jiang Y, et al (2012) Genetic analysis and molecular mapping of a new powdery mildew resistant gene Pm46 in common wheat. Theoretical and Applied Genetics 125:967–973. https://doi.org/10.1007/s00122-012-1886-7

Glémin S, Scornavacca C, Dainat J, et al (2019) Pervasive hybridizations in the history of wheat relatives. Sci Adv 5:. https://doi.org/10.1126/sciadv.aav9188

Gloss AD, Vergnol A, Morton TC, et al (2022) Genome-wide association mapping within a local Arabidopsis thaliana population more fully reveals the genetic architecture for defensive metabolite diversity. Philosophical Transactions of the Royal Society B: Biological Sciences 377:. https://doi.org/10.1098/rstb.2020.0512

Govta N, Polda I, Sela H, et al (2022) Genome-Wide Association Study in Bread Wheat Identifies Genomic Regions Associated with Grain Yield and Quality under Contrasting Water Availability. Int J Mol Sci 23:. https://doi.org/10.3390/ijms231810575

898 Haas M, Schreiber M, Mascher M (2019) Domestication and crop evolution of wheat and
899 barley: Genes, genomics, and future directions. J Integr Plant Biol 61:204–225.
900 https://doi.org/10.1111/jipb.12737

901 Han J, Zhang L-S, Li G-Q, et al (2009) Molecular Mapping of Powdery Mildew Resistance
902 Gene MlWE18 in Wheat Originated from Wild Emmer (Triticum turgidum var.
903 dicoccoides). ACTA AGRONOMICA SINICA 35:1791–1797.
904 https://doi.org/10.3724/sp.j.1006.2009.01791

905 Hao M, Liu M, Luo J, et al (2018) Introgression of powdery mildew resistance gene pm56 on
906 rye chromosome arm 6rs into wheat. Front Plant Sci 9:1040.
907 https://doi.org/10.3389/fpls.2018.01040

908 He H, Ji Y, Zhu S, et al (2017) Genetic, Physical and Comparative Mapping of the Powdery
909 Mildew Resistance Gene Pm21 Originating from Dasypyrum villosum. Front Plant Sci
910 8:1914. https://doi.org/10.3389/fpls.2017.01914

911 He H, Zhu S, Zhao R, et al (2018) Pm21, Encoding a Typical CC-NBS-LRR Protein, Confers
912 Broad-Spectrum Resistance to Wheat Powdery Mildew Disease. Mol Plant 11:879–
913 882. https://doi.org/10.1016/j.molp.2018.03.004

914 Hewitt T, Müller MC, Molnár I, et al (2021) A highly differentiated region of wheat
915 chromosome 7AL encodes a *Pm1a* immune receptor that recognizes its corresponding
916 *AvrPm1a* effector from *Blumeria graminis*. New Phytologist 229:2812–2826.
917 https://doi.org/10.1111/nph.17075

918 Hinterberger V, Douchkov D, Lück S, et al (2022) Mining for New Sources of Resistance to
919 Powdery Mildew in Genetic Resources of Winter Wheat. Front Plant Sci 13:366.
920 https://doi.org/10.3389/fpls.2022.836723

921 Hsam SLK, Huang XQ, Zeller FJ (2001) Chromosomal location of genes for resistance to
922 powdery mildew in common wheat (Triticum aestivum L. em Thell.) 6. Alleles at the
923 Pm5 locus. Theoretical and Applied Genetics 102:127–133.
924 https://doi.org/10.1007/s001220051627

925 Hu TZ, Li HJ, Liu ZJ, et al (2008) Identification and Molecular Mapping of the Powdery
926 Mildew Resistance Gene in Wheat Cultivar Yumai 66. ACTA AGRONOMICA SINICA
927 34:545–550. https://doi.org/10.3724/sp.j.1006.2008.00545

928 Huang XQ, Hsam SLK, Zeller FJ (2002) Chromosomal location of genes for resistance to
929 powdery mildew in Chinese wheat lines Jieyan 94-1-1 and Siyan 94-1-2. Hereditas
930 136:212–218. https://doi.org/10.1034/j.1601-5223.2002.t01-1-1360306.x

931 IWGSC, Appels R, Eversole K, et al (2018) Shifting the limits in wheat research and breeding
932 using a fully annotated reference genome. Science (1979) 361:.
933 https://doi.org/10.1126/science.aar7191

934 Ji X, Xie C, Ni Z, et al (2008) Identification and genetic mapping of a powdery mildew
935 resistance gene in wild emmer (Triticum dicoccoides) accession IW72 from Israel.
936 Euphytica 159:385–390. https://doi.org/10.1007/s10681-007-9540-1

937 Jin Y, Xue F, Zhou Y, et al (2020) Fine-Mapping of the Powdery Mildew Resistance Gene
938 mlxbd in the Common Wheat Landrace Xiaobaidong. Plant Dis 104:1231–1238.
939 https://doi.org/10.1094/PDIS-07-19-1347-RE

940 Kale SM, Schulthess AW, Padmarasu S, et al (2022) A catalogue of resistance gene homologs
941 and a chromosome-scale reference sequence support resistance gene mapping in
942 winter wheat. Plant Biotechnol J 20:1730–1742. https://doi.org/10.1111/pbi.13843

943 Kaur N, Street K, Mackay M, et al (2008) Molecular approaches for characterization and use
944 of natural disease resistance in wheat. In: European Journal of Plant Pathology.
945 Springer, pp 387–397

946 Keilwagen J, Lehnert H, Berner T, et al (2022) Detecting major introgressions in wheat and
947 their putative origins using coverage analysis. Sci Rep 12:1908.
948 https://doi.org/10.1038/s41598-022-05865-w

949 Kim SH, Hong JK, Lee SC, et al (2004) CAZFP1, Cys2/His2-type zinc-finger transcription factor
950 gene functions as a pathogen-induced early-defense gene in Capsicum annuum. Plant
951 Mol Biol 55:883–904. https://doi.org/10.1007/s11103-004-2151-5

952 Kloppe T, Whetten RB, Kim S, et al (2023) Two pathogen loci determine *Blumeria graminis* f.
953 sp. *tritici* virulence to wheat resistance gene *Pm1a*. New Phytologist.
954 https://doi.org/10.1111/nph.18809

955 Knaus BJ, Grünwald NJ (2017) VCFR: a package to manipulate and visualize variant call
956 format data in R. In: Molecular Ecology Resources. Blackwell Publishing Ltd, pp 44–53

957 Koller T, Brunner S, Herren G, et al (2019) Field grown transgenic Pm3e wheat lines show
958 powdery mildew resistance and no fitness costs associated with high transgene
959 expression. Transgenic Res 28:9–20. https://doi.org/10.1007/s11248-018-0099-5

960 Kolodziej MC, Singla J, Sánchez-Martín J, et al (2021) A membrane-bound ankyrin repeat
961 protein confers race-specific leaf rust disease resistance in wheat. Nat Commun 12:1–
962 12. https://doi.org/10.1038/s41467-020-20777-x

963 Komáromi J, Jankovics T, Fábián A, et al (2016) Powdery Mildew Resistance in Wheat
964 Cultivar Mv Hombár is Conferred by a New Gene, PmHo. Phytopathology 106:1326–
965 1334. https://doi.org/10.1094/PHYTO-03-16-0152-R

966 Kunz L, Sotiropoulos AG, Graf J, et al (2023) The broad use of the Pm8 resistance gene in
967 wheat resulted in hypermutation of the AvrPm8 gene in the powdery mildew
968 pathogen. BMC Biol 21:29. https://doi.org/10.1186/s12915-023-01513-5

969 Li G, Cowger C, Wang X, et al (2019) Characterization of Pm65, a new powdery mildew
970 resistance gene on chromosome 2AL of a facultative wheat cultivar. Theoretical and
971 Applied Genetics 132:2625–2632. https://doi.org/10.1007/s00122-019-03377-2

Li M, Dong L, Li B, et al (2020a) A CNL protein in wild emmer wheat confers powdery mildew resistance. New Phytologist 228:1027–1037. https://doi.org/10.1111/nph.16761

Li Y, Shi X, Hu J, et al (2020b) Identification of a recessive gene PMQ conferring resistance to powdery mildew in wheat Landrace qingxinmai using BSR-seq analysis. Plant Dis 104:743–751. https://doi.org/10.1094/PDIS-08-19-1745-RE

Lillemo M, Asalf B, Singh RP, et al (2008) The adult plant rust resistance loci Lr34/Yr18 and Lr46/Yr29 are important determinants of partial resistance to powdery mildew in bread wheat line Saar. Theoretical and Applied Genetics 116:1155–1166. https://doi.org/10.1007/s00122-008-0743-1

Liu J, He Z, Rasheed A, et al (2017) Genome-wide association mapping of black point reaction in common wheat (Triticum aestivum L.). BMC Plant Biol 17:220. https://doi.org/10.1186/s12870-017-1167-3

Liu Y, Chen J, Yin C, et al (2023) A high-resolution genotype–phenotype map identifies the TaSPL17 controlling grain number and size in wheat. Genome Biol 24:1–28. https://doi.org/10.1186/s13059-023-03044-2

Loh YT, Martin GB (1995) The Pto bacterial resistance gene and the Fen insecticide sensitivity gene encode functional protein kinases with serine/threonine specificity. Plant Physiol 108:1735–1739. https://doi.org/10.1104/pp.108.4.1735

Lopes MS, El-Basyoni I, Baenziger PS, et al (2015) Exploiting genetic diversity from landraces in wheat breeding for adaptation to climate change. J Exp Bot 66:3477–3486. https://doi.org/10.1093/jxb/erv122

Luo PG, Luo HY, Chang ZJ, et al (2009) Characterization and chromosomal location of Pm40 in common wheat: a new gene for resistance to powdery mildew derived from Elytrigia intermedium. Theoretical and Applied Genetics 118:1059–1064. https://doi.org/10.1007/s00122-009-0962-0

Lutz J, Hsam SLK, Limpert E, Zeller FJ (1995) Chromosomal location of powdery mildew resistance genes in triticum aestivum L. (common wheat). 2. genes pm2 and pm19 from aegi/ops squarrosa L. Heredity (Edinb) 74:152–156. https://doi.org/10.1038/hdy.1995.22

Lutz J, Limpert E, Bartos P, Zeller FJ (1992) Identification of Powdery Mildew Resistance Genes in Common Wheat (Triticum aestivum L.). I. Czechoslovakian Cultivars. Plant Breeding 108:33–39. https://doi.org/10.1111/j.1439-0523.1992.tb00097.x

Mackay M, Street K (2004) Focused identification of germplasm strategy — FIGS. In: Proceedings of the 54th Australian Cereal Chemistry Conference and the 11th Wheat Breeders' Assembly. Cereal Chemestry Division, Royal Australian Chemical Institute (RACI), Melbourne, Victoria, Australia., pp 138–141

1008 Manser B, Koller T, Praz CR, et al (2021) Identification of specificity-defining amino acids of
1009 the wheat immune receptor Pm2 and powdery mildew effector AvrPm2. The Plant
1010 Journal 106:993–1007. https://doi.org/10.1111/tpj.15214

1011 Mantel N, Valand RS (1970) A Technique of Nonparametric Multivariate Analysis. Biometrics
1012 26:547. https://doi.org/10.2307/2529108

1013 Marees AT, de Kluiver H, Stringer S, et al (2018) A tutorial on conducting genome-wide
1014 association studies: Quality control and statistical analysis. Int J Methods Psychiatr Res
1015 27:. https://doi.org/10.1002/mpr.1608

1016 Marone D, Russo MA, Mores A, et al (2021) Importance of landraces in cereal breeding for
1017 stress tolerance. Plants 10:1267. https://doi.org/10.3390/plants10071267

1018 Martin GB, Brommonschenkel SH, Chunwongse J, et al (1993) Map-based cloning of a
1019 protein kinase gene conferring disease resistance in tomato. Science (1979) 262:1432–
1020 1436. https://doi.org/10.1126/science.7902614

1021 Mascher M, Schreiber M, Scholz U, et al (2019) Genebank genomics bridges the gap
1022 between the conservation of crop diversity and plant breeding. Nat Genet 51:1076–
1023 1081. https://doi.org/10.1038/s41588-019-0443-6

1024 Maxwell JJ, Lyerly JH, Srnic G, et al (2010) MlAB10 : A Triticum turgidum Subsp. dicoccoides
1025 Derived Powdery Mildew Resistance Gene Identified in Common Wheat. Crop Sci
1026 50:2261–2267. https://doi.org/10.2135/cropsci2010.04.0195

1027 McDonald BA, Linde C (2002) Pathogen population genetics, evolutionary potential, and
1028 durable resistance. Annu Rev Phytopathol 40:349–379.
1029 https://doi.org/10.1146/annurev.phyto.40.120501.101443

1030 McIntosh RA, Yamazaki Y, Dubcovsky J, et al (2013) Catalogue of Gene Symbols for Wheat.
1031 In: Komugi wheat genetic resources database. https://wheat.pw.usda.gov/GG3/wgc.
1032 Accessed 8 Mar 2023

1033 Mohler V, Bauer C, Schweizer G, et al (2013) Pm50: A new powdery mildew resistance gene
1034 in common wheat derived from cultivated emmer. J Appl Genet 54:259–263.
1035 https://doi.org/10.1007/s13353-013-0158-9

1036 Mohler V, Zeller FJ, Wenzel G, Hsam SLK (2005) Chromosomal location of genes for
1037 resistance to powdery mildew in common wheat (Triticum aestivum L. em Thell.). 9.
1038 Gene MlZec1 from the Triticum dicoccoides-derived wheat line Zecoi-1. Euphytica
1039 142:161–167. https://doi.org/10.1007/s10681-005-1251-x

1040 Mu Y, Gong W, Qie Y, et al (2022) Identification of the powdery mildew resistance gene in
1041 wheat breeding line Yannong 99102-06188 via bulked segregant exome capture
1042 sequencing. Front Plant Sci 13:3277. https://doi.org/10.3389/fpls.2022.1005627

1043 Müller K, Wickham H (2022) tibble: Simple Data Frames. https://CRAN.R-
1044 project.org/package=tibble

1045 Müller MC, Kunz L, Schudel S, et al (2022) Ancient variation of the AvrPm17 gene in
1046 powdery mildew limits the effectiveness of the introgressed rye Pm17 resistance gene
1047 in wheat. Proc Natl Acad Sci U S A 119:e2108808119.
1048 https://doi.org/10.1073/pnas.2108808119

1049 Müller T, Schierscher-Viret B, Fossati D, et al (2018) Unlocking the diversity of genebanks:
1050 whole-genome marker analysis of Swiss bread wheat and spelt. Theoretical and
1051 Applied Genetics 131:407–416. https://doi.org/10.1007/s00122-017-3010-5

1052 Mundt CC (2014) Durable resistance: A key to sustainable management of pathogens and
1053 pests. Infection, Genetics and Evolution 27:446–455.
1054 https://doi.org/10.1016/j.meegid.2014.01.011

1055 Mundt CC (2018) Pyramiding for resistance durability: Theory and practice. Phytopathology
1056 108:792–802. https://doi.org/10.1094/PHYTO-12-17-0426-RVW

1057 Myles S, Peiffer J, Brown PJ, et al (2009) Association mapping: Critical considerations shift
1058 from genotyping to experimental design. Plant Cell 21:2194–2202.
1059 https://doi.org/10.1105/tpc.109.068437

1060 Niu JS, Wang BQ, Wang YH, et al (2008) Chromosome location and microsatellite markers
1061 linked to a powdery mildew resistance gene in wheat line Lankao 90(6). Plant Breeding
1062 127:346–349. https://doi.org/10.1111/j.1439-0523.2007.01480.x

1063 Oksanen J, Simpson Gavin L., Blanchet F. G., et al (2022) vegan: Community Ecology
1064 Package. https://CRAN.R-project.org/package=vegan. Accessed 25 May 2023

1065 Ouyang S, Zhang D, Han J, et al (2014) Fine Physical and Genetic Mapping of Powdery
1066 Mildew Resistance Gene MlIW172 Originating from Wild Emmer (Triticum
1067 dicoccoides). PLoS One 9:e100160. https://doi.org/10.1371/journal.pone.0100160

1068 Özkan H, Brandolini A, Schäfer-Pregl R, Salamini F (2002) AFLP Analysis of a Collection of
1069 Tetraploid Wheats Indicates the Origin of Emmer and Hard Wheat Domestication in
1070 Southeast Turkey. Mol Biol Evol 19:1797–1801.
1071 https://doi.org/10.1093/oxfordjournals.molbev.a004002

1072 Paux E, Lafarge S, Balfourier F, et al (2022) Breeding for Economically and Environmentally
1073 Sustainable Wheat Varieties: An Integrated Approach from Genomics to Selection.
1074 Biology (Basel) 11:149. https://doi.org/10.3390/biology11010149

1075 Pedersen TL (2020) patchwork: The Composer of Plots. https://CRAN.R-
1076 project.org/package=patchwork

1077 Perugini LD, Murphy JP, Marshall D, Brown-Guedira G (2008) Pm37, a new broadly effective
1078 powdery mildew resistance gene from Triticum timopheevii. Theoretical and Applied
1079 Genetics 116:417–425. https://doi.org/10.1007/s00122-007-0679-x

1080 Petersen S, Lyerly JH, Worthington ML, et al (2015) Mapping of powdery mildew resistance
1081 gene Pm53 introgressed from Aegilops speltoides into soft red winter wheat.

1082 Theoretical and Applied Genetics 128:303–312. https://doi.org/10.1007/s00122-014-
1083 2430-8

1084 Peusha H, Enno T, Priilinn O (2004) Chromosomal Location of Powdery Mildew Resistance
1085 Genes and Cytogenetic Analysis of Meiosis in Common Wheat Cultivar Meri. Hereditas
1086 132:29–34. https://doi.org/10.1111/j.1601-5223.2000.00029.x

1087 Praz CR, Bourras S, Zeng F, et al (2017) AvrPm2 encodes an RNase-like avirulence effector
1088 which is conserved in the two different specialized forms of wheat and rye powdery
1089 mildew fungus. New Phytologist 213:1301–1314. https://doi.org/10.1111/nph.14372

1090 Pugsley AT, Carter M V. (1953) The resistance of twelve varieties of triticum vulgare to
1091 erysiphe graminis tritici. Aust J Biol Sci 6:335–346. https://doi.org/10.1071/BI9530335

1092 Purcell S, Neale B, Todd-Brown K, et al (2007) PLINK: A tool set for whole-genome
1093 association and population-based linkage analyses. Am J Hum Genet 81:559–575.
1094 https://doi.org/10.1086/519795

1095 Qie Y, Sheng Y, Xu H, et al (2019) Identification of a new powdery mildew resistance gene
1096 pmDHT at or closely linked to the Pm5 locus in the Chinese wheat landrace
1097 dahongtou. Plant Dis 103:2645–2651. https://doi.org/10.1094/PDIS-02-19-0401-RE

1098 Qiu YC, Zhou RH, Kong XY, et al (2005) Microsatellite mapping of a Triticum urartu Tum.
1099 derived powdery mildew resistance gene transferred to common wheat (Triticum
1100 aestivum L.). Theoretical and Applied Genetics 111:1524–1531.
1101 https://doi.org/10.1007/s00122-005-0081-5

1102 R Core Team (2022) R: A language and environment for statistical computing.
1103 https://www.r-project.org/

1104 Reif JC, Zhang P, Dreisigacker S, et al (2005) Wheat genetic diversity trends during
1105 domestication and breeding. Theoretical and Applied Genetics 110:859–864.
1106 https://doi.org/10.1007/s00122-004-1881-8

1107 Rimbert H, Darrier B, Navarro J, et al (2018) High throughput SNP discovery and genotyping
1108 in hexaploid wheat. PLoS One 13:. https://doi.org/10.1371/journal.pone.0186329

1109 Robinson JT, Thorvaldsdóttir H, Winckler W, et al (2011) Integrative genomics viewer. Nat
1110 Biotechnol 29:24–26. https://doi.org/10.1038/nbt.1754

1111 Sánchez-Martín J, Keller B (2021) NLR immune receptors and diverse types of non-NLR
1112 proteins control race-specific resistance in Triticeae. Curr Opin Plant Biol 62:102053.
1113 https://doi.org/10.1016/j.pbi.2021.102053

1114 Sánchez-Martín J, Steuernagel B, Ghosh S, et al (2016) Rapid gene isolation in barley and
1115 wheat by mutant chromosome sequencing. Genome Biol 17:1–7.
1116 https://doi.org/10.1186/s13059-016-1082-1

1117 Sánchez-Martín J, Widrig V, Herren G, et al (2021) Wheat Pm4 resistance to powdery
1118 mildew is controlled by alternative splice variants encoding chimeric proteins. Nat
1119 Plants 1–15. https://doi.org/10.1038/s41477-021-00869-2

1120 Sansaloni C, Franco J, Santos B, et al (2020) Diversity analysis of 80,000 wheat accessions
1121 reveals consequences and opportunities of selection footprints. Nat Commun 11:4572.
1122 https://doi.org/10.1038/s41467-020-18404-w

1123 Sato K, Abe F, Mascher M, et al (2021) Chromosome-scale genome assembly of the
1124 transformation-amenable common wheat cultivar 'Fielder. DNA Research 28:.
1125 https://doi.org/10.1093/dnares/dsab008

1126 Savary S, Willocquet L, Pethybridge SJ, et al (2019) The global burden of pathogens and
1127 pests on major food crops. Nat Ecol Evol 3:430–439. https://doi.org/10.1038/s41559-
1128 018-0793-y

1129 Schulthess AW, Kale SM, Liu F, et al (2022) Genomics-informed prebreeding unlocks the
1130 diversity in genebanks for wheat improvement. Nat Genet 54:1544–1552.
1131 https://doi.org/10.1038/s41588-022-01189-7

1132 Sharma R, Mahanty B, Mishra R, Joshi RK (2021) Genome wide identification and expression
1133 analysis of pepper C2H2 zinc finger transcription factors in response to anthracnose
1134 pathogen Colletotrichum truncatum. 3 Biotech 11:118.
1135 https://doi.org/10.1007/s13205-020-02601-x

1136 Shi AN, Leath S, Murphy JP (1998) A major gene for powdery mildew resistance transferred
1137 to common wheat from wild einkorn wheat. Phytopathology 88:144–147.
1138 https://doi.org/10.1094/PHYTO.1998.88.2.144

1139 Singh BK, Delgado-Baquerizo M, Egidi E, et al (2023) Climate change impacts on plant
1140 pathogens, food security and paths forward. Nat Rev Microbiol 21:640–656

1141 Singh SP, Hurni S, Ruinelli M, et al (2018) Evolutionary divergence of the rye Pm17 and Pm8
1142 resistance genes reveals ancient diversity. Plant Mol Biol 98:249–260.
1143 https://doi.org/10.1007/s11103-018-0780-3

1144 Singrün C, Hsam SLK, Zeller FJ, et al (2004) Localization of a novel recessive powdery mildew
1145 resistance gene from common wheat line RD30 in the terminal region of chromosome
1146 7AL. Theoretical and Applied Genetics 109:210–214. https://doi.org/10.1007/s00122-
1147 004-1619-7

1148 Sotiropoulos AG, Arango-Isaza E, Ban T, et al (2022) Global genomic analyses of wheat
1149 powdery mildew reveal association of pathogen spread with historical human
1150 migration and trade. Nat Commun 13:16. https://doi.org/10.1038/s41467-022-31975-
1151 0

1152 Stein N, Herren G, Keller B (2001) A new DNA extraction method for high-throughput
1153 marker analysis in a large-genome species such as Triticum aestivum. Plant Breeding
1154 120:354–356. https://doi.org/10.1046/j.1439-0523.2001.00615.x

1155 Sun M, Liu Q, Han Y, et al (2022) PmSN15218: A Potential New Powdery Mildew Resistance
1156 Gene on Wheat Chromosome 2AL. Front Plant Sci 13:.
1157 https://doi.org/10.3389/fpls.2022.931778

1158 Tan C, Li G, Cowger C, et al (2019) Characterization of Pm63, a powdery mildew resistance
1159 gene in Iranian landrace PI 628024. Theoretical and Applied Genetics 132:1137–1144.
1160 https://doi.org/10.1007/s00122-018-3265-5

1161 Tan C, Li G, Cowger C, et al (2018) Characterization of Pm59, a novel powdery mildew
1162 resistance gene in Afghanistan wheat landrace PI 181356. Theoretical and Applied
1163 Genetics 131:1145–1152. https://doi.org/10.1007/s00122-018-3067-9

1164 Tanksley SD, McCouch SR (1997) Seed banks and molecular maps: Unlocking genetic
1165 potential from the wild. Science (1979) 277:1063–1066.
1166 https://doi.org/10.1126/science.277.5329.1063

1167 Tettelin H, Masignani V, Cieslewicz MJ, et al (2005) Genome analysis of multiple pathogenic
1168 isolates of Streptococcus agalactiae: Implications for the microbial "pan-genome."
1169 Proc Natl Acad Sci U S A 102:13950–13955. https://doi.org/10.1073/pnas.0506758102

1170 Tian Z-D, Zhang Y, Liu J, Xie C-H (2010) Novel potato C2H2-type zinc finger protein gene,
1171 StZFP1, which responds to biotic and abiotic stress, plays a role in salt tolerance. Plant
1172 Biol 12:689–697. https://doi.org/10.1111/j.1438-8677.2009.00276.x

1173 Tosa Y, Tsujimoto H, Ogura H (1987) A gene involved in the resistance of wheat to
1174 wheatgrass powdery mildew fungus. Genome 29:850–852.
1175 https://doi.org/10.1139/g87-145

1176 Uehara Y, Takahashi Y, Berberich T, et al (2005) Tobacco ZFT1, a transcriptional repressor
1177 with a Cys2/His 2 type zinc finger motif that functions in spermine-signaling pathway.
1178 Plant Mol Biol 59:435–448. https://doi.org/10.1007/s11103-005-0272-0

1179 Uffelmann E, Huang QQ, Munung NS, et al (2021) Genome-wide association studies. Nature
1180 Reviews Methods Primers 1:1–21. https://doi.org/10.1038/s43586-021-00056-9

1181 Van Den Burg HA, Tsitsigiannis DI, Rowland O, et al (2008) The F-box protein
1182 ACRE189/ACIF1 regulates cell death and defense responses activated during pathogen
1183 recognition in tobacco and tomato. Plant Cell 20:697–719.
1184 https://doi.org/10.1105/tpc.107.056978

1185 Villa TCC, Maxted N, Scholten M, Ford-Lloyd B (2005) Defining and identifying crop
1186 landraces. Plant Genetic Resources 3:373–384. https://doi.org/10.1079/pgr200591

1187 Vleeshouwers VGAA, Oliver RP (2014) Effectors as tools in disease resistance breeding
1188 against biotrophic, hemibiotrophic, and necrotrophic plant pathogens. Molecular
1189 Plant-Microbe Interactions 27:196–206. https://doi.org/10.1094/MPMI-10-13-0313-IA

1190 Walkowiak S, Gao L, Monat C, et al (2020) Multiple wheat genomes reveal global variation
1191 in modern breeding. Nature 588:277–283. https://doi.org/10.1038/s41586-020-2961-
1192 x

1193 Wan W, Xiao J, Li M, et al (2020) Fine mapping of wheat powdery mildew resistance gene
1194 Pm6 using 2B/2G homoeologous recombinants induced by the ph1b mutant.
1195 Theoretical and Applied Genetics 133:1265–1275. https://doi.org/10.1007/s00122-
1196 020-03546-8

1197 Wang J, Li Y, Xu F, et al (2022) Candidate powdery mildew resistance gene in wheat
1198 landrace cultivar Hongyoumai discovered using SLAF and BSR-seq. BMC Plant Biol
1199 22:83. https://doi.org/10.1186/s12870-022-03448-5

1200 Wang J, Zhang Z (2021) GAPIT Version 3: Boosting Power and Accuracy for Genomic
1201 Association and Prediction. Genomics Proteomics Bioinformatics 19:629–640.
1202 https://doi.org/10.1016/j.gpb.2021.08.005

1203 Wang W, He H, Gao H, et al (2021) Characterization of the Powdery Mildew Resistance
1204 Gene in Wheat Breeding Line KN0816 and Its Evaluation in Marker-Assisted Selection.
1205 Plant Dis 105:4042–4050. https://doi.org/10.1094/PDIS-05-21-0896-RE

1206 Wei T, Simko V (2021) R package "corrplot": Visualization of a Correlation Matrix.
1207 https://github.com/taiyun/corrplot

1208 Weigel RR, Pfitzner UM, Gatz C (2005) Interaction of NIMIN1 with NPR1 modulates PR gene
1209 expression in Arabidopsis. Plant Cell 17:1279–1291.
1210 https://doi.org/10.1105/tpc.104.027441

1211 Wenger AM, Peluso P, Rowell WJ, et al (2019) Accurate circular consensus long-read
1212 sequencing improves variant detection and assembly of a human genome. Nat
1213 Biotechnol 37:1155–1162. https://doi.org/10.1038/s41587-019-0217-9

1214 Wickham H (2016) ggplot2: Elegant Graphics for Data Analysis. Springer-Verlag New York

1215 Wickham H, François R, Henry L, et al (2023) dplyr: A Grammar of Data Manipulation.
1216 https://CRAN.R-project.org/paclage=dplyr

1217 Worthington M, Lyerly J, Petersen S, et al (2014) *MlUM15* : an *Aegilops neglecta* -derived
1218 Powdery Mildew Resistance Gene in Common Wheat. Crop Sci 54:1397–1406.
1219 https://doi.org/10.2135/cropsci2013.09.0634

1220 Wu L, Zhu T, He H, et al (2022) Genetic dissection of the powdery mildew resistance in
1221 wheat breeding line LS5082 using BSR-Seq. Crop Journal 10:1120–1130.
1222 https://doi.org/10.1016/j.cj.2021.12.008

1223 Wu P, Hu J, Zou J, et al (2019) Fine mapping of the wheat powdery mildew resistance gene
1224 Pm52 using comparative genomics analysis and the Chinese Spring reference genomic
1225 sequence. Theoretical and Applied Genetics 132:1451–1461.
1226 https://doi.org/10.1007/s00122-019-03291-7

1227 Xiao M, Song F, Jiao J, et al (2013) Identification of the gene Pm47 on chromosome 7BS
1228 conferring resistance to powdery mildew in the Chinese wheat landrace Hongyanglazi.
1229 Theoretical and Applied Genetics 126:1397–1403. https://doi.org/10.1007/s00122-
1230 013-2060-6

1231 Xie JZ, Wang L li, Wang Y, et al (2017) Fine mapping of powdery mildew resistance gene
1232 PmTm4 in wheat using comparative genomics. J Integr Agric 16:540–550.
1233 https://doi.org/10.1016/S2095-3119(16)61377-1

1234 Xing L, Hu P, Liu J, et al (2018) Pm21 from Haynaldia villosa Encodes a CC-NBS-LRR Protein
1235 Conferring Powdery Mildew Resistance in Wheat. Mol Plant 11:874–878.
1236 https://doi.org/10.1016/j.molp.2018.02.013

1237 Xu H, Yao G, Xiong L, et al (2008) Identification and mapping of pm2026: A recessive
1238 powdery mildew resistance gene in an einkorn (Triticum monococcum L.) accession.
1239 Theoretical and Applied Genetics 117:471–477. https://doi.org/10.1007/s00122-008-
1240 0791-6

1241 Xu W, Li C, Hu L, et al (2011) Identification and molecular mapping of PmHNK54: a novel
1242 powdery mildew resistance gene in common wheat. Plant Breeding 130:603–607.
1243 https://doi.org/10.1111/j.1439-0523.2011.01882.x

1244 Xu WG, Li CX, Hu L, et al (2010) Molecular mapping of powdery mildew resistance gene
1245 PmHNK in winter wheat (Triticum aestivum L.) cultivar Zhoumai 22. Molecular
1246 Breeding 26:31–38. https://doi.org/10.1007/s11032-009-9374-8

1247 Xu X, Li Q, Ma Z, et al (2018) Molecular mapping of powdery mildew resistance gene PmSGD
1248 in Chinese wheat landrace Shangeda using RNA-seq with bulk segregant analysis.
1249 Molecular Breeding 38:1–12. https://doi.org/10.1007/s11032-018-0783-4

1250 Xu X, Liu W, Liu Z, et al (2020) Mapping Powdery Mildew Resistance Gene pmYBL on
1251 Chromosome 7B of Chinese Wheat (Triticum aestivum L.) Landrace Youbailan. Plant
1252 Dis 104:2411–2417. https://doi.org/10.1094/PDIS-01-20-0118-RE

1253 Xue F, Ji W, Wang C, et al (2012) High-density mapping and marker development for the
1254 powdery mildew resistance gene PmAS846 derived from wild emmer wheat (Triticum
1255 turgidum var. dicoccoides). Theoretical and Applied Genetics 124:1549–1560.
1256 https://doi.org/10.1007/s00122-012-1809-7

1257 Yahiaoui N, Srichumpa P, Dudler R, Keller B (2004) Genome analysis at different ploidy
1258 levels allows cloning of the powdery mildew resistance gene Pm3b from hexaploid
1259 wheat. The Plant Journal 37:528–538. https://doi.org/10.1046/j.1365-
1260 313X.2003.01977.x

1261 Yao G, Zhang J, Yang L, et al (2007) Genetic mapping of two powdery mildew resistance
1262 genes in einkorn (Triticum monococcum L.) accessions. Theoretical and Applied
1263 Genetics 114:351–358. https://doi.org/10.1007/s00122-006-0438-4

1264 Yin J, Wang L, Zhao J, et al (2020) Genome-wide characterization of the C2H2 zinc-finger
1265 genes in Cucumis sativus and functional analyses of four CsZFPs in response to
1266 stresses. BMC Plant Biol 20:359. https://doi.org/10.1186/s12870-020-02575-1

1267 Yin JL, Fang ZW, Sun C, et al (2018) Rapid identification of a stripe rust resistant gene in a
1268 space-induced wheat mutant using specific locus amplified fragment (SLAF)
1269 sequencing. Sci Rep 8:1–9. https://doi.org/10.1038/s41598-018-21489-5

1270 Yu X, Ren S, Zhao L, et al (2018) Molecular mapping of a novel wheat powdery mildew
1271 resistance gene Ml92145E8-9 and its application in wheat breeding by marker-assisted
1272 selection. Crop Journal 6:621–627. https://doi.org/10.1016/j.cj.2018.04.004

1273 Zeller FJ, Kong L, Hartl L, et al (2002) Chromosomal location of genes for resistance to
1274 powdery mildew in common wheat (Triticum aestivum L. em Thell.) 7. Gene Pm29 in
1275 line Pova. Euphytica 123:187–194. https://doi.org/10.1023/A:1014944619304

1276 Zeven AC (1998) Landraces: A review of definitions and classifications. Euphytica 104:127–
1277 139. https://doi.org/10.1023/A:1018683119237

1278 Zhan H, Li G, Zhang X, et al (2014) Chromosomal Location and Comparative Genomics
1279 Analysis of Powdery Mildew Resistance Gene Pm51 in a Putative Wheat-Thinopyrum
1280 ponticum Introgression Line. PLoS One 9:e113455.
1281 https://doi.org/10.1371/journal.pone.0113455

1282 Zhang D, Zhu K, Dong L, et al (2019) Wheat powdery mildew resistance gene Pm64 derived
1283 from wild emmer (Triticum turgidum var. dicoccoides) is tightly linked in repulsion
1284 with stripe rust resistance gene Yr5. Crop Journal 7:761–770.
1285 https://doi.org/10.1016/j.cj.2019.03.003

1286 Zhang H, Guan H, Li J, et al (2010) Genetic and comparative genomics mapping reveals that
1287 a powdery mildew resistance gene Ml3D232 originating from wild emmer co-
1288 segregates with an NBS-LRR analog in common wheat (Triticum aestivum L.).
1289 Theoretical and Applied Genetics 121:1613–1621. https://doi.org/10.1007/s00122-
1290 010-1414-6

1291 Zhang R, Fan Y, Kong L, et al (2018) Pm62, an adult-plant powdery mildew resistance gene
1292 introgressed from Dasypyrum villosum chromosome arm 2VL into wheat. Theoretical
1293 and Applied Genetics 131:2613–2620. https://doi.org/10.1007/s00122-018-3176-5

1294 Zhang R, Sun B, Chen J, et al (2016) Pm55, a developmental-stage and tissue-specific
1295 powdery mildew resistance gene introgressed from Dasypyrum villosum into common
1296 wheat. Theoretical and Applied Genetics 129:1975–1984.
1297 https://doi.org/10.1007/s00122-016-2753-8

1298 Zhang W, Yu Z, Wang D, et al (2023) Characterization and identification of the powdery
1299 mildew resistance gene in wheat breeding line ShiCG15–009. BMC Plant Biol 23:113.
1300 https://doi.org/10.1186/s12870-023-04132-y

1301 Zheng X, Levine D, Shen J, et al (2012) A high-performance computing toolset for
1302 relatedness and principal component analysis of SNP data. Bioinformatics 28:3326–
1303 3328. https://doi.org/10.1093/bioinformatics/bts606

Zhou X, Stephens M (2012) Genome-wide efficient mixed-model analysis for association studies. Nat Genet 44:821–824. https://doi.org/10.1038/ng.2310

Zhu Z, Zhou R, Kong X, et al (2005) Microsatellite markers linked to 2 powdery mildew resistance genes introgressed from Triticum carthlicum accession PS5 into common wheat. Genome 48:585–590. https://doi.org/10.1139/G05-016

Zhu Z, Zhou R, Kong X, et al (2006) Microsatellite marker identification of a Triticum aestivum-Aegilops umbellulata substitution line with powdery mildew resistance. Euphytica 150:149–153. https://doi.org/10.1007/s10681-006-9103-x

Zou S, Wang H, Li Y, et al (2018) The NB-LRR gene Pm60 confers powdery mildew resistance in wheat. New Phytologist 218:298–309. https://doi.org/10.1111/nph.14964

Statements & Declarations

Funding

This project was financially supported by the University of Zurich, Swiss National Science Foundation grants 310030_204165 and 310030B_182833 to B.K. JSM is recipient of the grants “Ramon y Cajal” Fellowship RYC2021-032699-I, funded by MCIN/AEI/10.13039/501100011033 and by the “European Union NextGenerationEU/PRTR”, and PID2022-142651OA-I00, funded by MCIN/AEI/10.13039/501100011033 and by the “European Union NextGenerationEU/PRTR”.

Competing Interests

Beat Keller is a member of the editorial board of TAG. The authors declare no other competing interests.

Author contribution statement

J.S.M. and B.K. conceived the project. E.J. and R.L. performed seed propagation. R.L., V.W. and J.S.M. performed infection tests. R.L. performed DNA extraction, PCR screens and allele detection. E.P. performed SNP array genotyping. R.L. and M.H. performed bioinformatics analysis. R.L., J.S.M. and B.K. analyzed the data and wrote the manuscript. All authors revised the manuscript.

Data Availability

1330 The mildew isolate CHE_19004 whole-genome sequence data is available at NCBI's Short Read Archive
1331 (SRA) under the accession code BioProject PRJNA945619. The nine isolate sequences from earlier work
1332 (Sotiropoulos et al. 2022) are available at NCBI under PRJNA625429 and SRP062198. The genotyping data
1333 of landraces from the study of Balfourier and colleagues (Balfourier et al. 2019) can be accessed at
1334 https://urgi.versailles.inra.fr/download/wheat/genotyping/Balfourier_et_al_Wheat_Phylogeography_D
1335 ataS2.zip. All other data needed to evaluate the conclusions in this study are included in the article and
1336 its supplementary information files. All *Blumeria graminis* f.sp. *tritici* isolates used in this study are kept
1337 alive in the Department of Plant and Microbial Biology of the University of Zurich and are available upon
1338 request.

1339

1340 **Supporting information captions**

1341 **Supplementary file1**

1342

1343 **Supplementary file2**

1344 **Table S1. Information on accessions of the LandracePlus panel.** Alleles with asterisks are non-functional. Groups
1345 are based on the hierarchical clustering of the LandracePLUS panel, including high-quality sequenced genomes.

1346

1347 **Table S2. Differential lines used for determining powdery mildew isolate virulence spectra and the respective**
1348 **Pm genes they contain.**
1349 NILs had been backcrossed multiple times with susceptible accessions “Federation” or “Chancellor”, depicted by
1350 /x*Accession, where x is the number of backcrosses to the designated accession (McIntosh et al. 2013).

1351

1352 **Table S3. Molecularly known Avr and Svr haplotypes of the ten powdery mildew isolates used for phenotyping.**
1353 H0 = published avirulent haplotype, H1 = published virulent haplotype, H2 = unpublished haplotype. Based on the
1354 phenotype of the differential lines containing cognate Pm genes, we propose that H2 of AvrPm1a and AvrPm3a/f
1355 are virulent, while H2 of AvrPm3d is proposed to be avirulent. H2 of AvrPm17 is likely virulent due to the
1356 resemblance of H1, with just one additional amino acid change. The resistant phenotype of the differential line
1357 containing Pm17 is suggested to be due to an additional Pm gene in Amigo. Amino acid (AA) changes are given
1358 based on H0 and depicted with original AA, position, new AA.

1359

1360 **Table S4. Heritability of phenotypes for all ten powdery mildew isolates based on a linear mixed model.**

1361

1362 **Table S5. Correlation of genetic relatedness and phenotypes for the ten *Bgt* isolates.**

1363

1364 **Table S6. Gene candidates and annotations in Chinese Spring for regions associated to powdery mildew**
1365 **resistance.** Highlighted genes are the best candidates based on their annotation.

1366

1367 **Table S7. List of all significantly associated SNPs, their position, MAF, effect size beta and p-values for the**
1368 **LandracePLUS panel excluding subsets.**

1369

1370 **Table S8. List of all significantly associated SNPs, their position, MAF, effect size beta and p-values for the**
1371 **subsets of the LandracePLUS panel.**

1372

1373 **Table S9. Raw phenotype data of the LandracePLUS panel infected with ten powdery mildew isolates.** Plates
1374 refer to the individual petri dish the replicate was in and Rounds to a batch that was infected at the same time.

1375

1376 **Supplementary file3**
1377 Alleles in the twenty most modern cultivars of the LandracePLUS panel for each potentially novel resistance-
1378 associated region. Resistance-associated alleles and accessions with more than 50% of these alleles and a
1379 resistance phenotype towards the peak-producing isolate are highlighted in bold.

1380

1381 **Dataset**
1382 **Data S1. Raw genotyping data of the LandracePLUS panel with the TaBW35K SNP array.** Empty cells are labelled
1383 "vide", and wheat accession IDs are extended by "_cell identifier".

1384

1385 **Data S2. Sample statistics of the raw genotyping data of the LandracePLUS panel.** Total numbers are labelled
1386 "nb" and percentage "pc".

1387

1388 **Data S3. Marker statistics of the raw genotyping data of the LandracePLUS panel.** Total numbers are labelled
1389 "nb" and percentage "pc".

1390